1-1-2011

Comparative Analysis of a Low-Speed Wind Tunnel Designed for Renewable Energy Applications

Craig A. Zehrung
Purdue University, czehrung@purdue.edu

Graduate School ETD Form 9
(Revised 12/07)

PURDUE UNIVERSITY
GRADUATE SCHOOL
Thesis/Dissertation Acceptance

This is to certify that the thesis/dissertation prepared

By Craig Allen Zehrung

Entitled
COMPARATIVE ANALYSIS OF A LOW-SPEED WIND TUNNEL DESIGNED FOR RENEWABLE ENERGY APPLICATIONS

For the degree of Master of Science

Is approved by the final examining committee:

Dr. Richard Mark French
Chair

Dr. Helen McNally

Dr. Rodney Handy

To the best of my knowledge and as understood by the student in the *Research Integrity and Copyright Disclaimer (Graduate School Form 20)*, this thesis/dissertation adheres to the provisions of Purdue University's "Policy on Integrity in Research" and the use of copyrighted material.

Approved by Major Professor(s): Dr. Richard Mark French

Approved by: Dr. James Mohler 7/22/2011
Head of the Graduate Program Date

Graduate School Form 20
(Revised 9/10)

PURDUE UNIVERSITY
GRADUATE SCHOOL

Research Integrity and Copyright Disclaimer

Title of Thesis/Dissertation:

COMPARATIVE ANALYSIS OF A LOW-SPEED WIND TUNNEL DESIGNED FOR RENEWABLE ENERGY APPLICATIONS

For the degree of Master of Science

I certify that in the preparation of this thesis, I have observed the provisions of *Purdue University Executive Memorandum No. C-22,* September 6, 1991, *Policy on Integrity in Research.**

Further, I certify that this work is free of plagiarism and all materials appearing in this thesis/dissertation have been properly quoted and attributed.

I certify that all copyrighted material incorporated into this thesis/dissertation is in compliance with the United States' copyright law and that I have received written permission from the copyright owners for my use of their work, which is beyond the scope of the law. I agree to indemnify and save harmless Purdue University from any and all claims that may be asserted or that may arise from any copyright violation.

Craig Allen Zehrung

Printed Name and Signature of Candidate

7/22/2011

Date (month/day/year)

*Located at http://www.purdue.edu/policies/pages/teach_res_outreach/c_22.html

COMPARATIVE ANALYSIS OF A LOW-SPEED WIND TUNNEL DESIGNED FOR RENEWABLE ENERGY APPLICATIONS

A Thesis

Submitted to the Faculty

of

Purdue University

by

Craig A. Zehrung

In Partial Fulfillment of the

Requirements for the Degree

of

Master of Science

August 2011

Purdue University

West Lafayette, Indiana

To my family and friends for their continued support throughout all of my endeavors.

ACKNOWLEDGMENTS

I would like to thank all of the individuals whom have helped me down this path. I would like to thank my family for the moral and mental support which helped me maintain a proper direction and focus. I especially want to thank Dr. Richard Mark French for picking me up when things looked like they were at the worst and for providing more academic support than many advisors are able. I would like to thank Dr. Michael Kane, Associate Professor in the department of CNIT at Purdue University for loaning me the computer on which the CFD analysis was performed. I would like to thank Brant Price in the department of CNIT at Purdue University for providing insight and help with the integrated circuitry that made controlling and testing the tunnel possible. I would also like to thank my friend and colleague, James Stratton, who served as a sounding board and extra set of hands during the construction and testing. Finally, I would like to thank everyone whom is not listed for providing shoulders on which I could lean, helping me maintain my sanity.

TABLE OF CONTENTS

Page

Page

LIST OF TABLES

LIST OF FIGURES

Figure Page

Figure Page

ABSTRACT

Zehrung, Craig A. M.S., Purdue University, August 2011. Comparative Analysis of a Low-Speed Wind Tunnel Designed for Renewable Energy Applications. Major Professor: Richard Mark French.

This thesis describes the design, testing, and validation of an open-circuit, mid-sized wind tunnel used for the teaching of undergraduate courses and testing of green energy wind turbines. This thesis uses computational fluid dynamics to determine theoretical values for flow of the wind tunnel which were statistically compared to actual values of fluid flow. An overall analysis of efficiency and effectiveness were also performed. However, aerodynamic testing of actual prototype turbines will not be covered in this thesis, as it does not concern the tunnels adherence to theoretical flow values.

CHAPTER 1. INTRODUCTION

1.1. Introduction

This chapter provides information on the research question at hand: why it is being asked, why it is significant, and what overall limitations and delimitations were involved. Also listed is an accumulation of key terms that are used throughout this thesis.

1.2. Background

Green energy is an ever growing concern within our society, cultures, and the world as a whole. Countries around our globe are working together to create initiatives which will reduce the amount of green house gasses emitted into the Earth's atmosphere. These gasses not only affect our own people and landscapes here in the United States; their effects can be witnessed throughout our planet as a whole. There are multiple forms of energy production which are being created and studied to lessen our dependence on fossil fuels and foreign oil.

One of the proposed alternatives to fossil fuel energy production, wind energy, has been increasingly implemented in Indiana for over the past ten years. Wind energy is clean, safe, and effective, making the most of the limited resources available for energy production around the Midwest United States. As a means of increasing the amount of energy able to be produced by a single turbine, new designs, features, and components are constantly being researched. To create next generation, high efficiency, wind turbines, extensive testing and modeling must be performed.

In order to test these next generation turbines, researchers have two main options available to them. The first of these two options is to conduct the research using computer-aided design, CAD, programs in conjunction with computational fluid dynamics, CFD, programming. This type of analysis is fairly robust and often yields results that are considered by researchers and industrialists to be theoretically accepted values. However, this type of analysis can often become lengthy and requires high end computing equipment that is capable of handling the complicated computations. The second form of green energy research analysis includes scale model testing within a wind tunnel. This type of testing is faster, often cheaper, and allows for maximum manipulation of the model and testing regimes.

1.3. Statement of Problem

There is a gap that exists within available equipment. This gap of equipment is such that specialized wind tunnels which are autonomous, easy to use, and durable enough for the purpose of teaching students, yet specialized, finely controlled, with enough precision to produce accurate results for the purpose of green energy research do not exist. Currently, available undergraduate research tunnels built by outside firms lack precision and control and generally do not contain an onboard data acquisition unit. These tunnels are often very expensive and are not able to be easily moved once installed.

1.4. Research Question

The question being analyzed in this thesis is: *given a wind tunnel of known dimensions and modular capabilities, is it possible to achieve sub-sonic flow with acceptable operating conditions that adhere to theoretical values obtained from computational fluid dynamics programming, within a laboratory budget of less than 6000 dollars?*

1.5. Significance of Problem

The aim of this thesis is to produce a feasible design for a cost effective mid-sized wind tunnel used for the purpose of teaching undergraduate students and the testing of green energy wind turbines.

To adhere to the teaching requirement, the tunnel must be able to be modular, due to the fact that it may be moved from laboratory to laboratory as needed. Also, integrated with the teaching requirement, the tunnel must be able to collect and produce real-time data that is able to be saved for further manipulation and calculations by each student. In order to adhere to the green energy research requirement, the tunnel must be able to accommodate both horizontal and vertical axis wind turbines. The tunnel must be able to be finely controlled and manipulated for each experiment. Finally, this tunnel must maintain a budget of no more than 6000 dollars. This budgetary requirement is to ensure that most universities and facilities will be able to afford such a design.

1.6. Statement of Purpose

The scope of this thesis is design, build, and test a mid-sized wind tunnel within the limits of an operating laboratory budget. This tunnel must produce adequate and efficient sub-sonic flow conditions. The tunnel is designed to accept and monitor the two most common types of wind turbines: horizontal and vertical axes. It is designed so that it is durable for undergraduate use, while maintaining precision for graduate and research uses.

This thesis is designed to allow the reader to view the researcher's approach to creating and testing of the aforementioned wind tunnel. The data which was collected and analyzed has been provided so that the reader can determine the strengths and weaknesses of the researcher's design. These strengths and weaknesses will allow other researchers to attain cost-effective, optimized designs to suit current and future endeavors of their own.

The theoretical velocity values were determined using the computational fluid dynamics (CFD) program, Algor, created by Autodesk. These theoretical values were compared to actual values obtained from an integrated data acquisition system, DAQ, attached to a differential pressure sensor. The readings were taken using a pitot tube and the velocities were calculated using Bernoulli's equation. These two sets of data were statistically analyzed using Statistical Analysis Software, SAS, created by SAS Institute Incorporated and provided by Purdue University. Finally, a budgetary analysis is given so that the researcher's adherence to the allotted budget can be determined.

1.7. Assumptions

This thesis will be carried out with the following assumptions:

1. A wind-tunnel for next generation green energy wind turbines is required for testing and validation.
2. Green energy turbines will provide the ability to lighten our dependence, as a society, on fossil fuels and reduce the total amount of greenhouse gasses which are emitted.
3. The data obtained from the computational fluid dynamics program, Algor, from Autodesk, is valid and accepted as theoretically true.

1.8. Limitations

This thesis will be tested and written with the following limitations:

1. A very short amount of time was allotted for the design and build process to be completed.
2. The total budget provided for this project has been limited to less than 6000 dollars.
3. The amount of space available for the build and testing has been limited to a small portion of an undergraduate laboratory, which is also used to conduct classes during the testing phase.

1.9. Delimitations

This thesis will be performed and written using the following delimitations:

1. The amenities provided by the administration and staff of the College of Technology at Purdue University in West Lafayette, Indiana.

2. A period of one semester to design and build the apparatus.

3. A subsequent period of one semester to test and perform the statistical analysis.

4. The computational fluid dynamics programs currently owned by Purdue University.

5. The statistical computational packages currently owned by Purdue University.

1.10. Definitions of Key Terms

boundary layer – "The region, close to the surface of a solid body, where the effects of viscosity produce an appreciable loss of total head" (Pankhurst & Holder, 1952, p.12). The "total head" can also be referred to as the pressure.

closed-circuit tunnel – "(A tunnel which) has … a continuous path for the air" (Pope, 1954, p.6).

contraction section and settling chamber – first section of an open-circuit wind tunnel containing a honeycomb screen through which the air flow enters and is able to be converted from turbulent to laminar flow, while becoming compressed before entry into the test section.

diffuser – third section of an open-circuit wind tunnel placed at the exit of the test section through which the air exits the tunnel. The exit end of the diffuser section is connected to the fan which powers the tunnel.

free-stream velocity – "The velocity of the undisturbed fluid relative to a body immersed in it" (Pankhurst & Holder, 1952, p.11).

Mach Number - "… the ratio of the speed of the fluid to the local speed of sound" (Pankhurst and Holder, 1952, p. 29).

open-circuit tunnel – "(A tunnel which) has no guided return of air" (Pope, 1954, p.6).

Reynolds Number – A ratio of the inertial forces of a fluid placed on an object over the viscous forces of the fluid; $R_e=(\rho Vl)/\mu$.

separation point – "The position at which the boundary layer leaves the surface of the solid body" (Pankhurst & Holder, 1952, p.13).

stagnation point – "A point at which the fluid is brought to rest" (Pankhurst & Holder, 1952, p.11). This can be any type of barrier which disrupts fluid flow causing the flow at the point to have a velocity equal to zero.

stagnation pressure – "The pressure at any stagnation point" (Pankhurst & Holder, 1952, p.11).

static pressure – "… force per unit area of an element (on a) surface parallel to the (direction) of flow" (Pankhurst & Holder, 1952, p.11).

subsonic flow – air flow with a Mach number less than 1.

test section – second section of an open-circuit wind tunnel in which items of interest are subjected to the air flow and response variable measurements are conducted.

1.11. Summary

This chapter has provided the researcher's statement of purpose, research question, and the significance of the research. It has also provided the assumptions, limitations, delimitations, and the defined scope; all of which outline the boundaries of the project. Some of the key terms used in the research have been listed along with a brief overview of the projects background. Within the next section a brief history of wind tunnel use is given in the literature review. This literature review also contains a brief use of computational fluid dynamics programming and data acquisition integration.

CHAPTER 2. REVIEW OF RELEVANT LITERATURE

2.1. Introduction and Review

An extensive and detailed review of literature regarding wind tunnel design and their subsequent operation is challenging, since design rules are nearly impossible to set. Most wind tunnels are designed and built according to the test sections which they will be accommodating and the tests they will be performing. Many pieces of the information found and referenced in this chapter, as well as the next, provide data and results of successful designs constructed by other researchers to perform measurements within their specific fields. These successful designs have been adapted in the creation of the wind tunnel outlined in this thesis. One very close account of implementing strict guidelines for construction has come from Mehta and Bradshaw (1979), whom themselves have stated, “It is difficult and unwise to lay down firm design rules mainly because of the wide variety of requirements and especially the wide variety of working-section configurations” (p.443). However, successful past wind tunnel designs have been, many are not completely applicable to the type of tunnel being outlined in this document. Thus, they have been viewed as loose guidelines only. This review covers a short history of wind tunnel uses and their requirements along with the importance of wind tunnels in past and present research. This review also contains information on computational fluid dynamics, CFD, analyses and data acquisition, DAQ, devices.

2.2. Historic Aerodynamic Methods

Wind tunnels have been used for a multitude of years and gained a great deal of accreditation within the aeronautical and astronautical communities. Rae and Pope (1984) gave a brief overview of humanity's obsession with flight and their desire to design apparatuses in or on which flying vessels could be tested:

> The earliest attempts by humans to design heavier-than-air machines, or airplanes, was based on the observations of birds in flight. Most of these machines used flapping wings (orinthopters) powered by humans through various mechanisms. In the 15th century Leonardo da Vinci used this approach, among others, and he left a legacy of over 500 sketches and 35,000 words dealing with the problem of flight. All of the attempts at flight by human-powered orinthopters were failures. By the 18th and 19th centuries it was realized that our knowledge of what we now call aerodynamics was miniscule. This led to the concept of building instrumented facilities to measure aerodynamic forces and moments (p. 1).

Some of the first attempts to test aerodynamics utilized a whirling arm onto which an airfoil was attached. These attempts were effective but still flawed as the wing would pass through its own disturbed wake and yielding erroneous results and artificial lift conditions; thus leading to the need and development of further refined instruments and apparatuses (Rae & Pope, 1984). Pope (1947) has given a brief overview of the many methods used to obtain meaningful data from aerodynamic testing:

> Information useful for aerodynamic design may be obtained in a number of ways: from wind tunnels, rocket sleds, water tunnels, drops from aircraft, flying scale models, whirling arms, shock tubes, water tables, plunge barrels, rocket flights and ballistic ranges (p.1).

The definition of a wind tunnel as given by Pankhurst and Holder (1952), is, “A device for producing a moving airstream for experimental purposes...” (p.3). These tunnels were a vast improvement over the whirling arm designs as they could produce uniform and variably controlled air flows into which a model could be securely mounted and measured for reactions. However, it is noted that Pankhurst and Holder’s definition is vague as to the design constraints of size, scale, and number of sections required for such a device to be deemed a wind tunnel. This is due to the vast array of possibilities that have been utilized over the years. Most wind tunnels can be grouped into two main categories, open or return circuit tunnels. The test sections which they contain are also grouped into two main categories, open or closed jet. Due to these four simple choices in conjunction with fan types and overall dimensions, rarely are two tunnels constructed to be the exact same.

Open circuit wind tunnels, such as the depiction found in Figure 2.1 below, are those that draw their intake air from the surrounding room and exhaust it to the same. These tunnels do not contain any return passages through which the same air is passed back to the beginning of the contraction section. Rae and Pope (1984), whom refer to this type of tunnel as an Eiffel type, have listed the following advantages and disadvantages of such a tunnel, as quoted:

Advantages

1. Construction cost is less.
2. If one intends to run internal combustion engines or do much flow visualization via smoke, there is no purging problem if both inlet and exhaust are open to the atmosphere.

Disadvantages

1. If located in a room, depending on the size of the tunnel to the room size, it may require extensive screening at the inlet to get high-quality

flow. The same may be true if the inlet and/or exhaust is open to the atmosphere, when wind and cold weather can affect operation.

2. For a given size and speed the tunnel will require more energy to run. This is usually a factor only if used for developmental testing where the tunnel has a high utilization rate.
3. In general, a tunnel is noisy. For larger tunnels (test sections of 70 sq. ft. and more) noise may cause environmental problems and limits on hours of operation (p.10).

It has been noted in some cases, rooms which contain open circuit tunnels have been outfitted with turning vanes and baffles, which allow the room itself to act as a closed loop tunnel return.

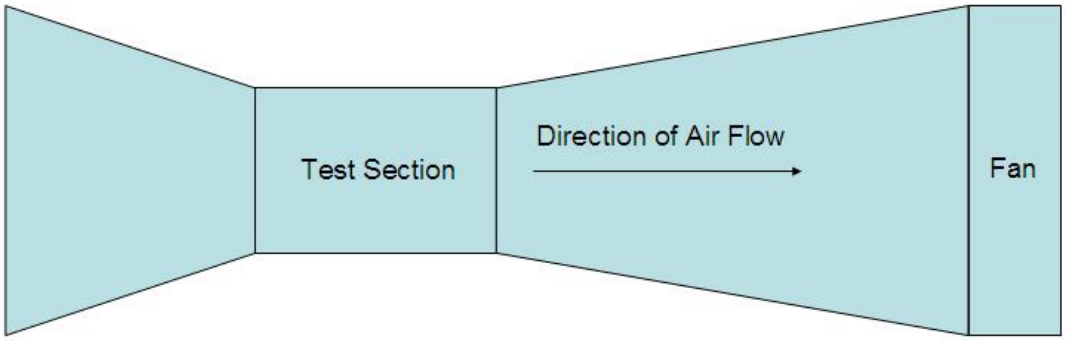

Figure 2.1 Depiction of an open circuit wind tunnel: This type of tunnel does not contain any return circuit through which the air is fed back into the contraction section.

Closed circuit wind tunnels, such as the depiction found in Figure 2.2 below, are those that contain a continuous loop from the diffuser section back to the contraction section. Minimal amounts of fresh air are drawn in from its surroundings. This type of tunnel can have a multitude of configurations and air return paths. Some tunnels operated by the National Aeronautics and Space Administration, NASA, contain a closed loop tunnel with an attached open loop tunnel, feeding its exhaust into the closed loop of the second tunnel. Rae and Pope (1984), whom refer closed loop tunnels as Göttingen-type tunnels, have listed the following advantages and disadvantages of such a tunnel, as quoted:

Advantages

1. Through the use of corner turning vanes and possibly screens, the quality of the flow can be easily controlled.
2. Less energy is required for a given test-section size and velocity. This can be important for a tunnel used for developmental testing with high utilization (two or three shifts, five to six days a week).
3. Less noise when operating.

Disadvantages

1. Higher initial costs due to return ducts and corner vanes.
2. If used extensively for smoke tests or running of internal combustion engines, there must be a way to purge tunnel.
3. If tunnel has high utilization, it may have to have an air exchanger or some other method of cooling during hot summer months (p.10).

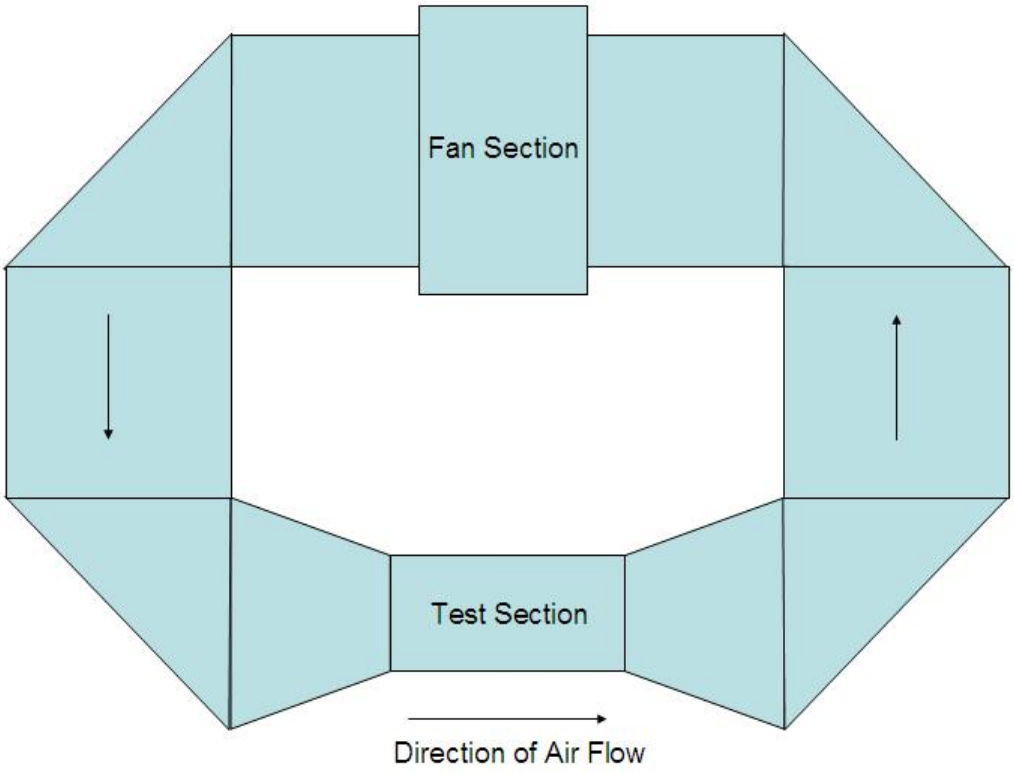

Figure 2.2 Depiction of a closed circuit wind tunnel: This type of tunnel contains a return loop from the end of the diffuser section back to the beginning of the contraction section.

Roberts (1961) has given the following statement which provides a brief description on open versus closed-jet test sections:

> Either of these wind tunnels may be designed with an “open jet” test section, in which the jet of the test section air is bounded by the still air of a room surrounding the jet, or by a closed jet test section which is bounded by the walls of a constant section between the exit of the contraction cone and the inlet of the diffuser (p.11).

Roberts went on to state that when considering the choices between the two, open-jet sections are generally only chosen when a large amount of freedom of the test section is required. Due to the large amounts of energy lost by the non-continuous walls, a more powerful fan should be used to make-up for said losses. Also the contraction and diffuser sections must be designed in such a way that the air is not able to become turbulent from the loss of boundaries.

Due to the higher construction costs and much larger dimensions required by closed loop tunnels, an open loop tunnel equipped with a closed-jet test section has been specified as the best suited type for undergraduate education and green energy applications within a university setting.

2.2.1. Historic Military Advancements

During World War II, aircraft development and prototyping was at an all time high. In order to validate each new aircraft design, engineers needed a means of testing these designs and recording the forces they would experience in flight to determine control characteristics, stability, and maneuverability. Since creating a full-scale model that may not meet the desired design specifications is expensive, costly, and was often approached foolishly, engineers began designing scale models to be tested in wind tunnels to observe the effects of the fluid's motion around the model. This was possible through the concept of relative motion. Pankhurst and Holder (1952) have described the concept of relative motion, "It may be shown that the flow pattern around a body depends on the relative motion, and is the same whether the body is moving through a fluid at rest or is held stationary in a moving stream…" (p.3). This relative motion statement was the backbone of wind tunnel testing as it states that in order to test the aerodynamic attributes of a model; the model does not have to move through the air. The air may be moved around the model. Since nearly every aspect of the testing could be controlled using a wind tunnel, test engineers could

augment and transition the design to simulate yaw, climb, and diving conditions (Pankhurst & Holder, 1952).

It was during this period in time that aerodynamic testing within the United States grew leaps and bounds. During this war effort, both sides, the Axis and the Allies, were trying to create more maneuverable and advanced fighters, as well as, more aerodynamic and longer flight bombers than the other. This arms race was well known at that time and still continues throughout the world today. This race for more efficient and faster airplanes in turn led to more efficient and specialized wind tunnels.

During the World War II effort, the constantly increasing air speeds realized with each new generation of fighter plane required wind tunnels that could produce faster air velocities. Near the end of the war, airplanes were reaching speeds of Mach 1.0. The Mach number of an air craft is described by Pankhurst and Holder (1952) as, "… the ratio of the speed of the fluid to the local speed of sound" (p. 29). Thus a Mach number of unity would signify that the speed of the air craft, or the speed of the air moving around the craft, has reached the speed of the propagation of the sound waves for given conditions. It was noted that aircrafts approaching a Mach number of unity would often experience extreme instability and produce flight conditions that were not linearly predictable. Lan and Roskam (1981) have given a brief overview of this phenomenon, "… if the flow velocity exceeds the propagation of speed of disturbances, these disturbances will pile up to form strong waves, called shock waves. These shock waves in turn produce large changes in flow properties" (pps.21-22). Lan and Roskam later mentioned that this large change in flow would produce a dramatically increased amount of drag on the aircraft which in turn caused instability.

After the war, researchers were still fascinated with this strange phenomenon that aircrafts experience when nearing and exceeding speeds of Mach 1. Once again, this lead to a further refinement of aircraft designs which in turn would set the way for newer generations of wind tunnels. These newer wind tunnels, using means that will not be covered in this thesis as they are lengthy and do not pertain to this researcher's design, were able to reach super and hyper sonic velocities; a monumental advancement. Since that time, researchers have developed multitudes of specialized tunnels to test nearly any condition which an object in flight will experience.

2.3. Current State of Tunnel Testing

Though bigger wind tunnels were thought to be better methods of production and testing in the past, these larger wind tunnels have started to become very expensive to maintain. Roberts (1961) noted that an increase in the use of smaller scale wind tunnels would become critical, "The small wind tunnel is expected to play an important part in relieving the load on larger wind tunnels and expediting the completion of otherwise low priority investigations" (p.1). These 'low priority investigations' have now become much more important in the post war era, where power generation is of a much larger concern than at that time. Since many larger tunnels have been forced to shut down due to overwhelming operating costs and maintenance fees, full-scale testing is being eliminated in lieu of computer testing and design. This new computer testing is the basis of research and design regarding large commercial and military aircrafts.

As described by Mecham (2003) NASA was forced to close four of its largest wind tunnels and transfer the operation of another to a university due to operating and maintenance costs. The first two tunnels, as listed by Mecham,

were located at NASA's Ames research facility and formed the National Full-Scale Aerodynamic Complex, NFAC. These tunnels had a combined operating cost of over twelve million dollars a year. They are listed as an eighty by one hundred and twenty foot tunnel, used most recently to test the military's F-18 and the commercial 737, and a forty by eighty foot tunnel. These tunnels, which shared the same power source, were, according to Mecham, "… regarded as the largest wind tunnel test section in the world" (p.40). Mecham has listed that the forty by eighty foot tunnel was built in 1944 and was primarily used to test World War II aircraft during its early years. The third tunnel forced shut down at the Ames Research Facility was a twelve foot pressure tunnel. This apparatus was capable of producing Reynolds numbers of twelve million per foot and was often used to test take-off and landing models

The final closed tunnel listed by Mecham was Langley's sixteen foot transonic tunnel. This tunnel was most notably used in the testing of the Bell X-1 and the Apollo spacecraft. The fifth tunnel, listed by Mecham, was fortunate enough to remain in operation. This was Langley's thirty by sixty foot tunnel whose use has been transferred to Old Dominion University and is being used to test automotive models for the National Association of Stock Car Auto Racing, NASCAR. However, these five tunnels were not the only NASA owned facilities to encounter problems. In 2001 Langley's sixteen foot transonic tunnel was shut down for a one million dollar repair after an incident when a portion of an engine model broke free during testing and severely damaged the tunnel. This accident forced NASA to shut down four other separate tunnels to evaluate test procedures and tunnel stabilities (n.a., 2001).

The shut down of the larger tunnels in recent years, as cited by low work loads and high operating costs, has allowed mid-sized wind tunnels, such as the one listed in this thesis, to find a very comfortable niche. Many universities, whom do not have the proximity and budget to operate larger tunnels like Old

Dominion, have started constructing wind tunnels of their own to test scale models and perform experiments. Roberts (1961) was keen to the requirements of universities and their research needs as early and the 1960's. This is found in the following statement:

> It has been apparent for some time, therefore, that there is a great and increasing need for small economic wind tunnels which would lighten the load on existing wind tunnels and permit the initiation of pure research and educational programs. These programs, unfortunately, have been severely curtailed due to the relatively low priority assigned to them. It is expected that more and more high schools and college curriculums will include courses in experimental aerodynamics and will need small, economic wind tunnels to provide laboratory demonstrations and research facilities for such courses (p.6).

During the era in which Roberts wrote this, it was true that universities were ranked very low in testing priorities at many major facilities. However, this statement of a need for smaller wind tunnels by universities still holds very true to today. Kubesh and Allie (2009) constructed a mid-sized wind tunnel with a test section of approximately 4.5 cubic feet for their undergraduate meteorological laboratory with the total cost just under 2500 dollars. Kubesh and Allie's situation was very similar to the restrictions placed on the wind tunnel in this thesis. Their goal was to create an operable wind tunnel within a confined space, under monetary restrictions, for the purposes of undergraduate education. Though their tunnel was much smaller in scale than the one defined in this thesis, the information is still very valid. Due to their monetary restrictions, they were not able to purchase a commercial wind tunnel. They have stated, "Researching commercially available wind tunnels for educational use, we found them to be far more expensive than we could afford…" Instead of constructing their tunnel from common supplies, they opted to have one built by a heating and ventilation

company. Using this ductwork tunnel, they found a source of power from a fan designed for barn ventilation, much like the fan used in this thesis.

The use of CFD analysis has greatly impacted wind tunnel and aerodynamics testing as a whole. This type of analysis has mostly ended the era of full-scale testing, but has yet to put an end to flight and university testing.

2.4. Computational Fluid Dynamics Testing

Many research and design firms are using CFD programming to predict efficiencies and reactions of their designs as they would be experienced in real world testing. In many cases, CFD analyses have been overtaking wind tunnel testing as the primary means of determining model reactions, as mentioned in the section above. Studt (2004) noted, “Computational fluid dynamics (CFD) simulation tools, first commercially developed in the late-1960’s, for similar flow situations were initially verified with wind tunnel results.” Once perfected, these CFD analyses have become the standard of theoretical results. Studt later stated, “… CFD performance, especially in the area of computationally complex turbulent flow regimes, has improved to the point where it can now be used as a primary design tool in the flow-related designs, eliminating the need for most wind tunnel testing…”

CFD testing is a very powerful and useful tool when the proper amount of time is allotted and funding is available for equipment. These types of analyses allow researchers to analyze scenarios which are otherwise unable to be tested, such as space shuttle re-entry where Mach numbers can be in excess of 20. Laurentiu (2004) has noted, “Computational fluid dynamics has grown rapidly… One of the reasons for CFD’s widespread growth is that its application in the manufacturing industry often leads to shortened design cycles and improved process performance” (p.43). Many of the programs which are used to predict

flow conditions are lengthy and require vast amounts of computer power to solve. Blazewicz, Kurowski, Ludwiczak, and Napierala (2010) have stated, "… (the) CFD problem is very complex and needs a lot of computational power to obtain the results in a reasonable time" (p.1301). The article written by Blazewicz et al. addresses the use of multiple computers being linked to one another to share the problem solving assignments.

The time required to solve CFD algorithms is dependant on the mesh size and type of analysis chosen for the model. Two types of meshing approaches are available. Meshes can be created over the surface of a model or inversely the fluid within or around the model may be meshed to determine its reaction when encountering the surface of the model. In the case of this thesis, the fluid itself is to be meshed rather than the part being meshed. Also noted in this case is that the walls of the model, which are the outer bounds of the fluid, are essentially being meshed as the boundary though they are not shown in the analysis. A mesh's size is strictly determinate on the quality of results the individual performing the analysis desires, versus the amount of time available to perform said analysis. Each point of the meshed grid represents an element which will be affected by the external flow and pressure forces. The greater the number of points chosen, the greater amount of time required to calculate the velocity and pressure effects from the surrounding meshed grid. The meshed grid is required in order to allow the simulation to create an approximate solution to the Navier-Stokes equation. Blazewicz et al. have described the computational requirements in the following statement:

> To perform the computations … a mathematical model has to be discretized and represented as a set of numerical procedures… Each part of the mesh represents a small quantum of the fluid defined by two variables: velocity and pressure. These parameters are iteratively

> computed for the whole mesh by simulating the fluid in the next period of time (t+∂t) (p.1301).

While very useful, these programs can not always fully predict and mimic actual operating conditions due to the high complexity of the programming. Tests as performed by Chamorrow and Porte-Agel (2010) depict how a boundary layer build-up, similar to that formed by the Earth's atmosphere, can affect the total efficiency of a wind turbine farm as a whole. Because the turbulence created by each individual turbine can have adverse effects on the surrounding turbines, advanced studies need to be performed using empirical testing. This empirical need greatly rests with the inabilities of computer software to account for the turbulence and variability in flow conditions cause by each surrounding turbine in conjunction with the variance of the wind conditions. A very similar result was determined by Howell, Qin, Edwards, and Durrani (2010) whose data from a two dimensional CFD program could not predict the actual operating conditions within a wind tunnel. A further 3-D CFD design allowed for a closer approximation, but did not completely mirror the experimental data. Many CFD programs lack the ability to model the various mechanical aspects of the designs, such as variable pitch blade angles and bearing drag within the electric motors (Howell et al, 2010).

While CFD modeling is quite useful, not all departments within a university are capable of purchasing the large amounts of computing equipment required to perform the analyses within set class times. In the case of this thesis, a cheaper and easier-to-use testing device was desired; thus the need for a wind tunnel. Also, due to ever changing undergraduate classes and CFD packages, requiring students to have an expansive, yet quickly learned, knowledge base of CFD operation is not practical.

2.5. Adaptation of Wind Tunnel Use for Green Energy

Just as airplanes can be tested in wind tunnels to simulate flight conditions, green energy wind turbines can tested to determine blade designs, gear housings, and overall efficiencies as well. The two main types of green energy turbines used in today's industry are horizontal and vertical axis turbines, often referred to as (HAWT) and (VAWT) respectively. Green energy is an ever growing field of research all around the globe. According to Howell et al. (2010), the European Union alone had pledged to harvest 12% of their total energy consumption from renewable resources by 2010. Due to the restricted amount of space available for wind turbines, compact and more efficient designs are vital. In order to create and validate these new generations of compact designs, a means of testing is required.

In order to properly test scale models of such turbines, the researcher conducting the experiment must be able to account for real-world flow conditions. This is done through the use of Reynolds Number matching. Due to the low speed conditions of the tunnel, the air is considered incompressible. Thus meaning that the density is unaffected by the velocity. Pankhurst and Holder (1952) have stated the following regarding low speed tunnels and subsequent Reynolds Numbers, "Thus, provided that the Reynolds numbers of the model experiment and full-scale flight are equal, a difference in velocity is unimportant" (p.35). Lan and Roskam (1981) have stated, "… difference(s) in Reynolds number between wind tunnel and full-scale flight, the model boundary layer characteristics will not correctly simulate those of the full scale airplane thereby creating some obvious variations in aerodynamic forces" (p.69). Thus it will be vital during actual green energy applications testing for the researcher to know the value of the tunnel's Reynolds number so that their model can be accurately tested. However, due to the low speed conditions, a true Reynolds number matching is nearly impossible within a tunnel of this type. Since many of the models which will be tested are on the order of $1/50^{th}$ of the true size, the speeds

within the tunnel would have to be fifty times the actual velocities experienced by a full model. In order to perform Reynolds number matching, a tunnel would have to produce velocities of Mach 2 or higher.

Since larger tunnels are enormously expensive to operate and construct, a smaller wind tunnel designed for the testing of these applications is required. Also, due to the large cost of computers and CFD packages able to perform proper analyses, it is impractical for a university wishing to teach a semester long course on green energy testing and analysis to purchase multiple sets of equipment for each student. Therein lies the requirement for a mid-sized, low-speed, autonomous wind tunnel.

2.6. Data Acquisition System Integration

To gain accurate and trustworthy data from a testing apparatus, a proper data acquisition system, DAQ, is required (Smith, 2002). Since most renewable energy research is being performed at the university level, and technological advances have provided data retrieval systems that are smaller than most calculators, a simple and integrated DAQ could be easily built into the overall structure of a mid-sized wind tunnel. A new generation of plug-and-play wind tunnels could drastically improve the overall testing, data retrieval, efficiency, and reliability. Due to the integration of all of the hardware and software, an entire wind tunnel has the ability to remain mobile, allowing for transport and testing. Small bench-top wind tunnels, available to for the testing of micro electro-mechanical systems, MEMS, and computer devices, which are portable, accurate, often including a DAQ, do not offer the ability to test larger designs (Hoske, 2009). Many bench-top tunnels are unable to accurately predict the characteristics of full sized models. Since the delicacy of such scaled-down models is high, there is an inability to attach measurement devices to the models. It has also been noted that testing models at such low Reynolds numbers, can

produce erroneous results. These devices are best suited for heat dissipation studies rather than aerodynamic pursuits.

Though many universities are constructing smaller scaled tunnels for research and investigative purposes, many of them such as the one outlined by Kubesh and Allie (2009), do not have incorporated data acquisition equipment. Their design, which is used to test measurement equipment intended for measuring meteorological attributes, did not mention any on-board DAQ. When designing a tunnel that is intended for the education of undergraduates, it is very effective if that tunnel is completely autonomous. In this manner, neither students nor the instructor are required to provide any further hardware other than instrumentation that may not already included.

2.7. Summary

A new wind tunnel design for green energy investigations and undergraduate understanding of wind tunnel operation and green energy concepts is needed. This tunnel should contain an on board DAQ and be able to stand completely autonomous from any other objects. This tunnel should also have the ability to be moved from laboratory to laboratory, providing that enough space in available, so that it may be able to change with the class schedule and requirements. The use of larger wind tunnels for aerodynamic designs and testing has been greatly diminished. Many of these larger tunnels have been shut down due to drastically increased CFD analysis. However, CFD analysis for a beginning program within a university department is not feasible due to the large amount of computers required to perform the analyses and cost of software packages.

CHAPTER 3. DESIGN AND METHODOLOGY

3.1. Introduction

This section of the thesis will outline the design and construction of the wind tunnel. Overall dimensions and build techniques have been established for the reader. The electronics and sensors used to obtain empirical data are outlined with a small inclusion of the programming used to collect the values. The computational fluid dynamics, CFD, programming used for validation of the tunnel as a whole has been listed. Included with this CFD outline, the researcher has given successful and unsuccessful methods which were encountered. Finally, the statistical methodology of the study has been described. The results of the statistical analysis can be found in chapter 5 of this thesis.

3.2. Wind Tunnel Construction

For this thesis, an open return wind tunnel was chosen due to dimensional restrictions from the allotted space provided for the construction and testing along with the monetary conditions of the project. The open return was chosen due to the fact that closed return wind tunnels are vastly larger and cost more to construct. A pull through design was chosen over a blow through design in order to decrease the amount of possible turbulence within the test section. Blow through designs require larger settling chambers and many more screens to straighten the path of the air. A closed jet test section was chosen over an open jet test section due to the extra power and dimensional requirements of an open jet design. The overall design of the tunnel within this thesis was based off of the

desired dimensions for the test section. The dimensions for the test section were determined to be two feet high by two feet wide by three feet long.

Dimensions for the subsequent contraction and diffuser sections have been outlined. These dimensions are based on guidelines provided by Mehta & Bradshaw (1979) as well as guidelines described by Roberts (1961). These guidelines were taken into account so that this researcher could produce adequate laminar test section flow. From these aforementioned test section dimensions, the contraction section was first section to be designed and built. The second section built was the diffuser, and the last was the test section. However, for the purpose of this thesis, the construction methodologies for each of these sections will be listed in order from the front of the wind tunnel to the back with the screen and fan listed last.

3.2.1. Contraction Section Construction

The contraction and settling chamber, which comprise the first section of the wind tunnel, will be referred to as the contraction section for the entirety of this portion of the thesis. The shape for the contraction section was chosen from the latter of the two most conventional methods of producing a successful contraction section: the “by eye” method in which the designer uses their best judgment and fine tunes the flow through a series of adjustments, or the mathematical approach where the researcher assigns a polynomial to define the shape. These two methods have been outlined by Mehta and Bradshaw (1979). The overall length of the contraction section was determined by researcher to be five feet. This length was set due to the restrictions of the total length of the room in which the tunnel was to be built and tested.

The opening of the contraction section was determined to be five feet wide by five feet tall. This value was based off of the laboratory's ceiling height and design guidelines established by Mehta and Bradshaw (1979) who sated, "… contraction ratios between about 6 and 9 are normally used." Due to a ceiling height of eight feet, and the center line of the tunnel being four feet from the floor, it was the goal of this researcher to stay towards the lower end of the ratio guidelines. Thus, the tunnel's contraction ratio is 6.25. The shape of this section was defined by the fifth ordered polynomial given below in Figure 3.1. This shape was chosen as it allowed for a simplified and precisely defined shape and ease of repetition between each of the internal panels comprising the contraction section.

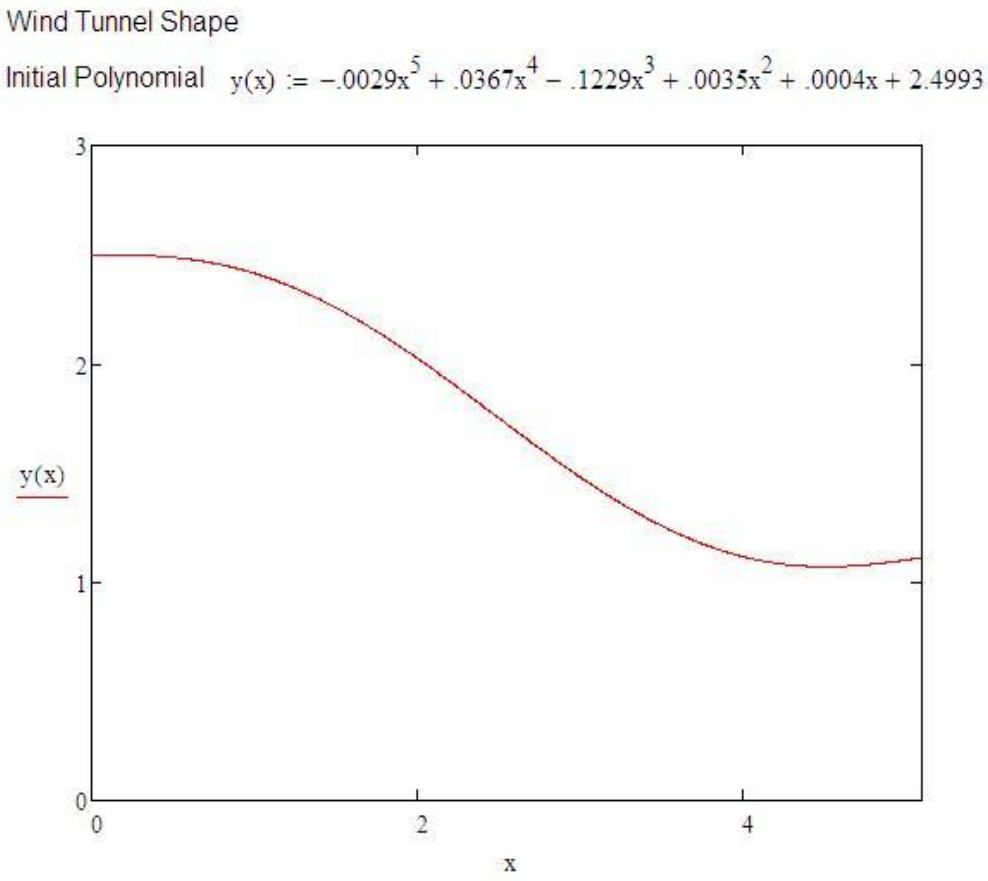

Figure 3.1 Fifth ordered polynomial line used to describe the shape of the contraction section.

The polynomial was created by assigning the first and last end points of the line, the first point being closest to the contraction section inlet, which was (0,2.5) and the last being near the test section inlet, (5,1). Each of these points represents the distance from the origin, set as the center of the contraction section, in feet. The next point added was the midpoint between the two end points, (2.5,1.75). A “best fit” fifth ordered polynomial curve was added using Microsoft Excel. While the equation given for the line is not an exact representation of the final shape, due to slight discontinuities near the test section side, adjustments were made during the fabrication processes to create an accurate fit.

The frame for the contraction section, as well as each of the other sections, was constructed using conventional two by fours. The frame for this section was comprised of five individual supports. Each support was constructed so that the inner faces contained the appropriate slope of the polynomial line at their respective points along the contraction section’s length. This slope was calculated by taking the derivative of the polynomial line at each respective point along the length of the section, with the beginning and end points having a slope of zero. Figure 3.2 below contains the derivative of the line and the slopes of each support. By incorporating the slope within each brace, an allowance for a reduction of discontinuities within contraction section panels was achieved along with an increase in structural rigidity due to the flush interface of each panel with its support. The corners of the supports were braced using square blocks cut from oriented strand board and secured with wood screws. The supports were evenly spaced and connected to one another using horizontal braces as shown in Figure 3.3 below. The legs of first two and last two sections of the frame, parallel to the tunnel’s length, were joined with one another to provide increased rigidity and platforms on which rollers, for ease of movement, and leveling feet, for stability during use, could be attached. Small leveling indicators were also added to the cross supports near each roller. Leveling indicators were also

added to the front and rear supports near the inlet and exit of the section. These indicators were added to aid in the assembly process. Due to dimensional conformity and rigidity, each section must be level before it is able to mount flush to the next section. Figure 3.4 below depicts the cross braces which were added between the legs of the supports and their accommodating hardware.

1st Derivative:

$$dy(x) := \frac{d}{dx} y(x) \rightarrow 0.007 \cdot x + -0.3687 \cdot x^2 + 0.1468 \cdot x^3 + -0.0145 \cdot x^4 + 0.0004$$

Spacing Interval:

$x := 0, 1.25 .. 5$

x =	y(x) =	dy(x) =
0	2.499	$4 \cdot 10^{-4}$
1.25	2.346	-0.316
2.5	1.752	-0.559
3.75	1.176	-0.284
5	1.101	0.105

+

Internal Support Angle Calculation:

FirstSupport := atan(0.0) = 0

SecondSupport := atan(−0.316)·57.3 = −17.538

ThirdSupport := atan(−0.559)·57.3 = −29.207

FourtSupport := atan(−0.284)·57.3 = −15.856

FifthSupport := atan(0.105)·57.3 = 5.995

Figure 3.2 Derivative of the polynomial line used to determine the internal angles of each support.

Figure 3.3 Contraction section frame: Each support was evenly spaced with varying internal angles according to their position along the contraction section's length.

Figure 3.4 Platforms added between the legs of the contraction section: providing a mounting surface on which rollers, leveling feet, and level indicators could be added.

Each internal side of the contraction section is comprised of three panels constructed from ¼ inch thick plywood. This approach was chosen to minimize the amount of time required to construct each side and to ensure that a proper fit between panels was achieved. Slight deformities were experienced due to the frame's natural tendency to warp since it was constructed of wood. Therefore, separate adjustments had to be made to accommodate for this shifting. Though the overall shape of the contraction section reflects the original polynomial curve given in Figure 3.2 above, each of the panels had to be cut using a longer, transformed, polynomial curve. This transformed polynomial curve was created to compensate for the extra distance each panel would have to cover due to the

distance lost by the curvature of each panel along the x and y axes. This second curve was created by performing a transform on the original curve to compensate for this loss of length. This transformation can be seen in Figure 3.5 below.

1st Derivative:

$$dy(x) := \frac{d}{dx} y(x) \rightarrow 0.007 \cdot x + -0.3687 \cdot x^2 + 0.1468 \cdot x^3 + -0.0145 \cdot x^4 + 0.0004$$

Side length transform with respect to x: $s(x) := \int_0^x \sqrt{dy(x)^2 + 1}\, dx$

X interval: $x := 0, .2 .. 5$

x =	y(x) =	s(x) =
0	2.499	0
0.2	2.499	0.2
0.4	2.493	0.4
0.6	2.479	0.601
0.8	2.453	0.802
1	2.414	1.006
1.2	2.361	1.213
1.4	2.295	1.424
1.6	2.216	1.639
1.8	2.125	1.858
2	2.025	2.082
2.2	1.919	2.309
2.4	1.808	2.537
2.6	1.696	2.766
2.8	1.587	2.994
3	1.482	3.22
3.2	1.384	3.443
3.4	1.297	3.661
3.6	1.223	3.874
3.8	1.162	4.083
4	1.117	4.288
4.2	1.087	4.491
4.4	1.073	4.691
4.6	1.072	4.891
4.8	1.083	5.092
5	1.101	5.292

Figure 3.5 Polynomial transform: required to account for the linear loss of length experience by each of the contraction section panels.

The first two panels placed in each internal side of the frame were the farthest ends containing the stretched polynomial shape. The sides opposite of these non-linear edges were cut so that they would be linear. This allowed for the third, middle portion, of each side to compensate for any shifting that would occur during the fit and installation of the first two panels. Figure 3.6 below displays the contraction section after all of the panels were installed. If the non-linear sides were cut to the exact stretched polynomial curve and the fit of the pieces within the frame was exact, the central portion would in-turn be an exact rectangle. However, this was often not the case and trapezoidal shapes were cut for compensation. The polynomials were cut using a template, which was printed to scale using a large scale plotter, and transferred onto each corresponding panel. A jig saw was used to cut each of the curved sides. In order to ensure that the edges opposite of the polynomials were linear, a circular saw was used.

Figure 3.6 Contraction section once the panels were installed.

Minimization of boundary layer build-up within a wind tunnel's test section is important so that flow separation and turbulent disruptions are not induced into the flow. Minimization of this build-up is also important so that velocities may remain constant throughout the length of the test section. If a boundary layer is able to build up within a test section, it has the ability to cause a choking effect which in turn causes an increase in pressure and disrupts the velocity. These types of increases can often lead to artificial lift conditions within the test section and produce erroneous test results.

The concept of a boundary layer was first introduced by Ludwig Prandtl in 1904. This concept was introduced as a solution to conformity issues between mathematical data and empirical testing data (Curle, 1962). The mathematical models of that time were using the concept of the inviscid theory. This theory stated that fluid did not contain any noteworthy viscous effects. Curle (1962) was noted for saying, “that according to inviscid theory any body moving uniformly through an unbound homogeneous fluid will experience zero drag!” (p.1). This concept of zero drag was the basis for Prandtl’s theory. Schlichting (1960) recounted Prandtl’s presentation before the Mathematical Congress:

> He proved that the flow about a solid body can be divided into two regions: a very thin layer in the neighborhood of the body (*boundary layer*) where friction plays an essential part and the remaining region outside this layer, where friction may be neglected (p.1).

This new theory, which included Euler’s original inviscid theory, helped pave the way for modern fluid dynamics research. This viscous layer, that presents itself near an object’s surface as it passes through a flow, is created by the flow of the fluid having a net velocity of zero at the surface. This zero velocity is cause by the viscous effects of the fluid as a whole. This viscous layer approaches the free stream velocity asymptotically. Over a large distance, the boundary layer is able to continue building upon itself until it finally separates from the surface. This separation is described by Curle (1962) in the passage below:

> When the fluid is proceeding into a region of rising pressure, it is slowed down by the retarding force. In the outer part of the boundary layer, where the kinetic energy is large, this results only in a relatively slow back-flow be set up. In such circumstances the forward flow must leave the surface

> to by-pass this region, and boundary-layer separation is said to have taken place (p.2).

Due to the way which the walls meet at ninety degrees within the contraction section, it was thought early on that a boundary layer build-up in these areas could have the significant ability to separate and cause turbulence within the test section. Therefore, corner blocks were created and installed.

Once the panels were in place and fastened on all four internal sides of the contraction section, these corner blocks were added so that boundary layer build-up could be minimized. The corner blocks were designed so that they would decrease linearly along the length of the contraction section, ensuring that a discontinuity was not experienced at the inlet of the test section. These corner blocks were designed as triangular fillets with the hypotenuse having an initial length of 3.25 inches at the contraction section inlet, diminishing to zero inches at the inlet of the test section; providing a smooth transition for laminar flow. These blocks were cut from conventional two by fours using a custom made jig and a table saw, ensuring that each block was an isosceles triangle. A depiction of this jig is shown below in Figure 3.7. Three blocks were used per contraction section corner, to allow for easier installation. In order to shape the blocks so that their overall dimensions would decrease over their length, while allowing the angles to remain the constant, they were placed on a large belt sander. This was chosen so that material removal rates would remain low and the process could be easily controlled. After shaping the blocks to their final shape, small kerfing slits were placed along the back side every half inch and cut to varying depths so that the front face thickness would be 0.375 inches; leaving them rigid yet flexible enough to conform to the contour of the wall interfaces. Figure 3.8 below contains a picture of one of the corner blocks before being installed.

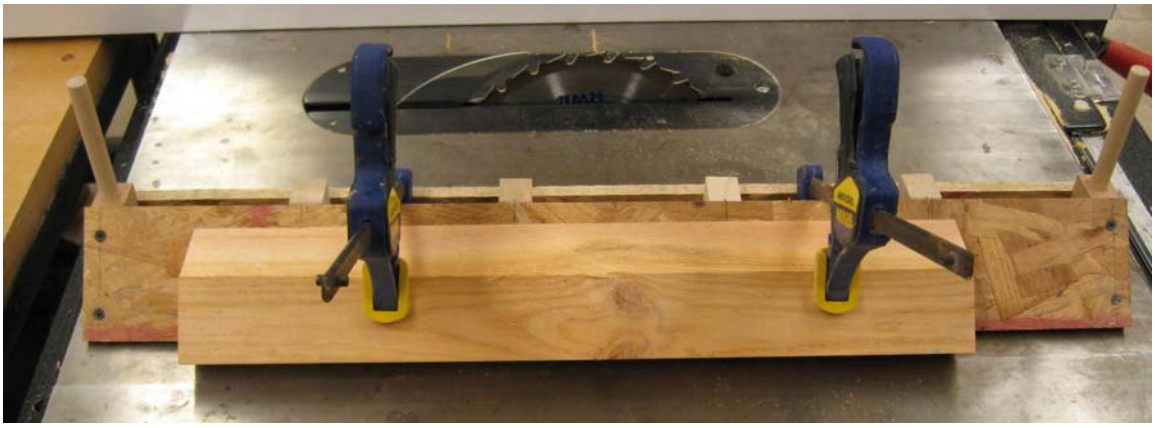

Figure 3.7 Jig created to cut the corner blocks installed in the contraction section.

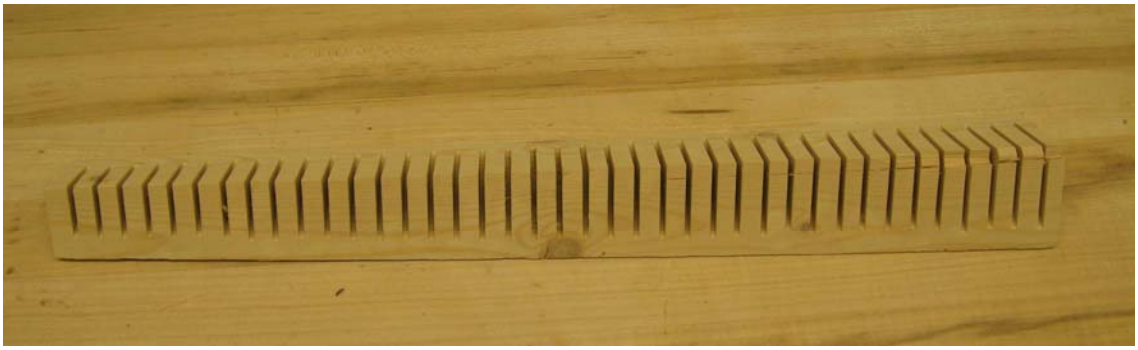

Figure 3.8 Corner block before installation.

After the installation of the corner blocks, a two-part epoxy resin infused with a micro-bubble fill was applied to the surface of the inner walls of the contraction section to smooth any discontinuities, cover all screw holes, and transition the corner blocks to the sides. This was done to produce uniform surfaces and eliminate areas which could produce disruptions. In order to determine the correct ratio of resin to micro-bubbles, four test pieces cut from extra paneling material were made and covered with the mixture. Each of these test pieces were graded by the researcher on appearance, amount of time required to dry, and their ability to be easily sanded. Figure 3.9 below is a depiction of each of these test pieces with varying resin and fill mixtures. Once a proper mixture was determined and applied, each side was hand sanded to

ensure that material removal was not excessive. A final sealant coating of shellac infused with wax was placed over top of the epoxy and bare wood to seal the wood from moisture. This final coating was initially hand sanded with a 440 grit sand paper to remove any runs or built up areas that occurred during application and was once again hand sanded using a semi-fine steel wool; providing a very smooth surface. Figure 3.10 below is a depiction of the contraction section once it was finished.

Figure 3.9 Test pieces with varying mixtures of a two-part epoxy resin and micro-bubble fill. Each was graded on appearance, dry time, and ability to be sanded.

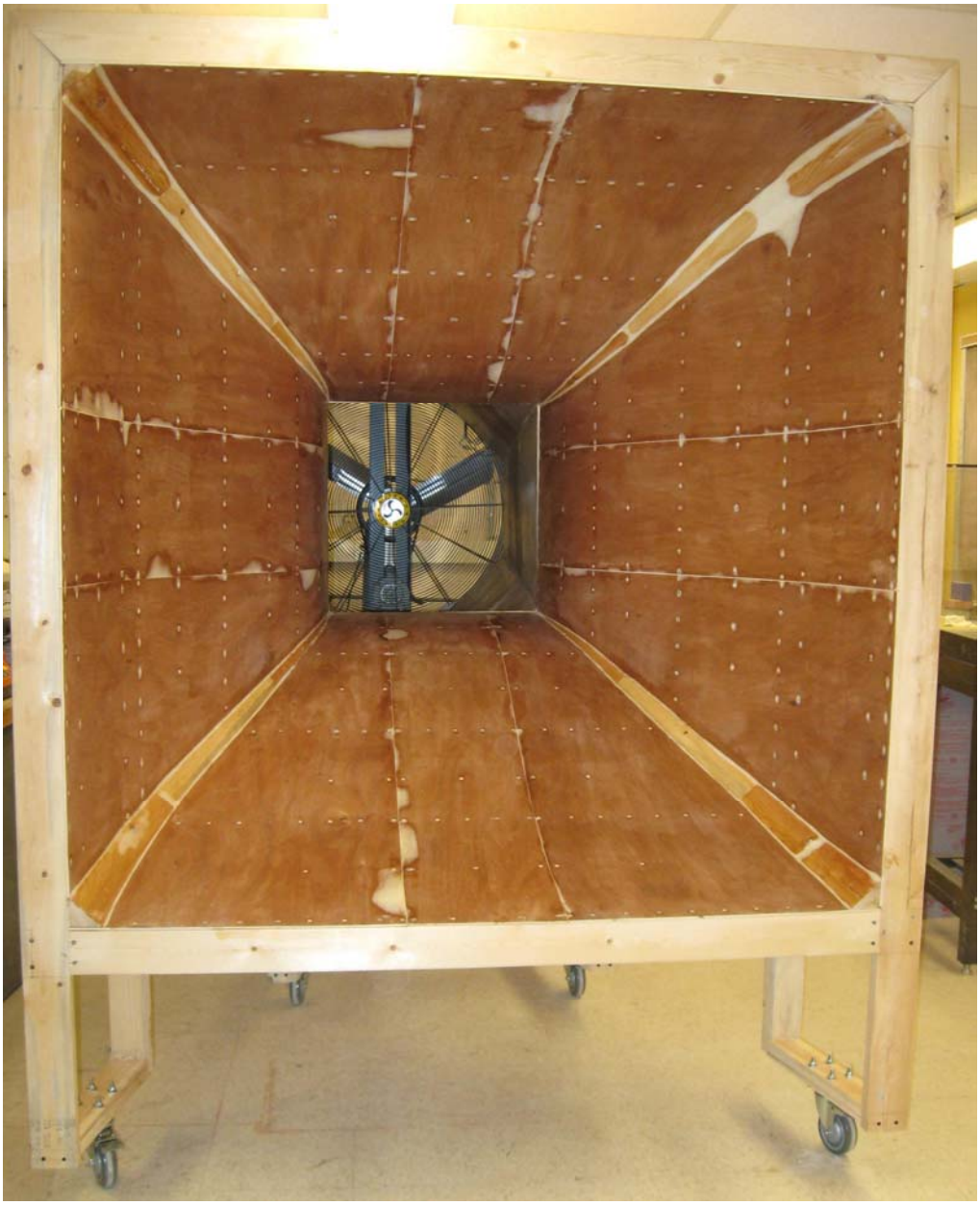

Figure 3.10 Contraction section once finished. The finished design contains the internal panels and corner fillets. The screw holes and discontinuities within the contraction section were filled with a two part epoxy resin. A final coating of shellac infused with wax was added. This final coat was hand sanded until a smooth finish was achieved.

3.2.2 Test Section Construction

The dimensions for the test section were initially set so that the inlet would be two feet wide by two feet tall with an overall length of three feet. The material chosen for the construction was 3/8 inch thick polycarbonate sheet. Polycarbonate provides the operator and spectators a three hundred and sixty degree view of the model as it is being tested, while maintaining safety in the case of accidental disruptions within the section during operation. Polycarbonate was chosen over Acrylic because it is much more ductile and less volatile when experiencing external forces, which may be applied during disassembly, movement, and reassembly of the tunnel. Since one of the requirements of the tunnel is that it be modular and able to be moved, Acrylic sheet posed the possibility of fracturing during this process.

Once the polycarbonate sheets were received, it was found that the overall dimensions were smaller than the dimensions ordered. Due to this unexpected anomaly, the width and height of the test section were altered to match the largest dimension able to be produced from the material, 23.5 inches. This dimension was achieved by overlapping the edge of each sheet onto the next sheet. Figure 3.11 below depicts how the sheets were joined with one another.

Within the top and bottom sheets of the test section, large counter bore holes were milled so that two large aluminum plates could be fitted into each. Initially, the two holes were to be created so that their major diameter would be twelve inches with a counter bore diameter of eleven inches. However due to the secondary overlapped design, a calculation was made in error which caused the center points of the two plates to be misaligned. To correct this misalignment, the top sheet was milled to contain a larger counter bored hole whose major diameter was 12.5 inches and minor diameter was 11.5 inches. This larger hole allowed the center of the top plate to become aligned with the center of the

bottom plate. The bottom sheet of the test section was also milled to contain degree markers so that the operator could rotate and position the test model to experience different angles of attack from the free stream flow. Each of these degree markers were placed five degrees apart from one another with larger marks every forty-five degrees. Figure 3.12 below is a depiction of the bottom sheet once milled. A handle was attached to the bottom plate so that the operator could easily turn and adjust the plate from outside of the test section, allowing for easier model manipulation during testing.

Figure 3.11 Joining of the test section sheets.

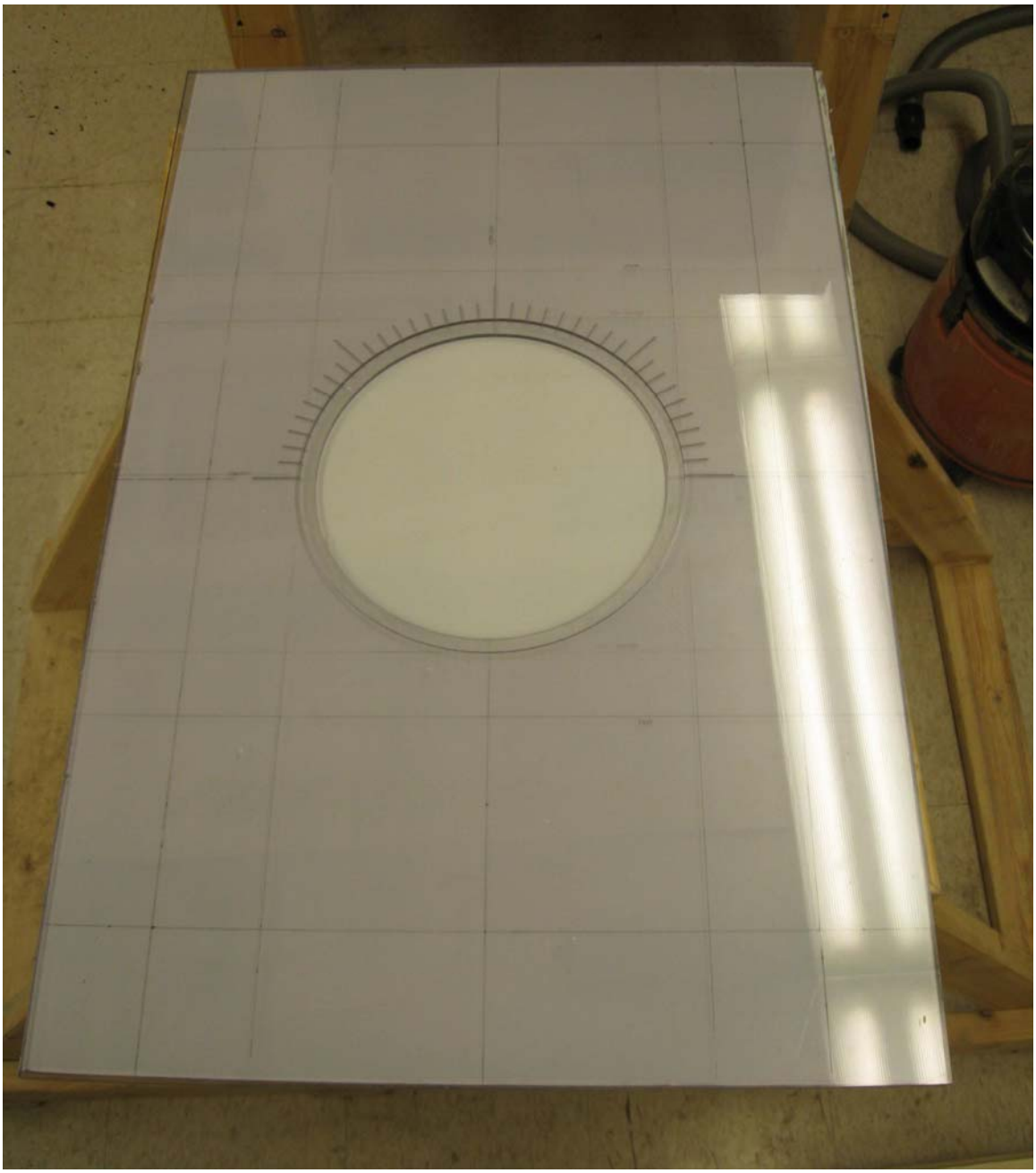

Figure 3.12 Test section bottom sheet: milled to contain a counter bore with a major diameter of twelve inches and a minor diameter of eleven inches into which an aluminum plate was placed.

The door to the test section underwent several design changes. The initial design was to include a set of hinges which would allow the door to swing upwards so that the operator could load and unload the models. However, this design was flawed as it would have caused an obstruction to the top plate and would require some sort of latch so that it would remain in place while opened. Also, a separate set of latches would have to be incorporated so that it would remain closed during movement. Therefore, a secondary design was created. This secondary design included two vertical polycarbonate supports which would be affixed between the top and bottom sheets. These supports would be added so that the top and bottom sheets would have stability and the test section door would be removable. The door and supports would be milled so that half of the thickness of each piece, 3/16 inch, by one half inch wide would be removed along the edge of their mating surface height. The supports and door would then be outfitted with flush mount magnets which would hold the door in place. This design was also abandoned as it was determined that the magnets would not have enough strength to hold the door in place. Since the strength of a magnet is based on its distance from the second surface, the total loss of force was great enough that it would not hold the polycarbonate door. A final design was decided upon in which the door and supports would remain yet the magnets would be replaced by a compression fitting between the top sheet of the test section and a piece of aluminum placed at the bottom. This piece of aluminum bracket was attached to the test section's stand through the use of ¼ inch diameter lag bolts. Figure 3.13 below is a depiction of the door and its subsequent mounting.

Figure 3.13 Test section door: held into place by a compression fit between the overlap of the test section's top sheet and an aluminum angle bracket affixed to the test section's stand.

Initially, the polycarbonate sheets were thought to have enough strength to support themselves so that only an aluminum angle bracket would have to be added to attach the test section to contraction and diffuser sections. However, this was not the case as the top and bottom sheets both lost a considerable amount of structural rigidity. This structural rigidity is accounted to the removal of material in order to accommodate the heavier aluminum plates. To solve this structural demand, corner braces were created and affixed to aluminum angle brackets to create a frame at either end of the test section. The polycarbonate sheets were attached to the frame using countersunk ¼-20 fasteners. Figure 3.14 below depicts the polycarbonate sheets affixed to the structural frame. Once the fasteners were in place, a piece of cellophane tape was placed over the holes for the fasteners inside of the test section to diminish any possibilities of flow disruptions. The aluminum frame was then equipped with ¼-20 carriage bolts, lock washers, and wing nuts which would allow the test section to be attached to the contraction and diffuser sections. In order to ensure that the carriage bolts would successfully mount within the wooden frames of the contraction and diffuser sections, steel anchor plates were added to the frames. Figure 3.15 below depicts these anchors and the mounting hardware used to attach the test section to each of the other two sections.

Figure 3.14 Structural test section frame: providing supports for the polycarbonate sheets and a mating surface between the test section and contraction and diffuser sections.

Figure 3.15 Mounting interface between the test section and the contraction and diffuser sections with carriage bolts and anchors.

The test section is supported by means of a wooden stand constructed of two by fours which serves two purposes. The first is to provide rigidity and proper height to the test section so that it can be mated to the other two sections and the second duty is to house the electronics and data acquisition hardware. The stand was designed to have a wide stance, lowering the center of gravity, so susceptibility to tipping from external forces during storage and transport would be diminished. The test section was attached to the stand using similar aluminum angle brackets used to attach the test section to the contraction and diffuser sections. The same counter sunk ¼-20 fasteners were used to attach the polycarbonate to the aluminum angle brackets and ¼ inch diameter lag bolts were used to attach the aluminum angle brackets to the stand. A piece of plywood was placed in the bottom of the stand so that equipment could be stored and secured during transportation. Similar to the contraction section's frame, the test section stand was equipped with rollers for movement, adjustable legs for stability during use, and leveling indicators. Figure 3.16 below is a depiction of the test section and its stand once it was completed.

Figure 3.16 Test section attached to stand with platform.

3.2.2. Diffuser Section Construction

The design for the diffuser section, much like the test section, went through several iterations before a final design was chosen. The inlet to this section was determined by the theoretical dimensions of the test section outlet, twenty-four inches wide by twenty-four inches tall. The diffuser section's exit dimension was set by the diametric dimension of the fan used to power the tunnel, forty-two inches. Mehta & Bradshaw (1979) established a general angular expansion guideline which states that the diffuser expansion angle should not exceed five degrees to avoid flow separation and turbulence. Taking this constraint into consideration, it was determined that the diffuser section should be seven feet long, thus creating an expansion angle of approximately 5.04 degrees. Figure 3.17 below depicts the calculations used to determine the angular expansion of the diffuser section. While the dimensions were set, a feasible design was still required.

Octagonal Major Diameter: $od := 38.75$

Inlet Height: $ih := 24$

Half of Height Change over Diffuser Section Length: $hh := \frac{(od - ih)}{2} = 7.375$

Diffuser Section Total Length: $dl := 84$

Expansion Angle: $ea := \left(\tan\left(\frac{hh}{dl}\right)\right)57.3 = 5.044$

Figure 3.17 Diffuser expansion angle calculation.

The entrance of the diffuser was set to a two foot by two foot square, while the exit of the diffuser needed to accommodate a forty-two inch circular fan. The initial design was to create overlapping panels which would allow for a smooth transition from a square to a circle. However, this design would prove to be time

consuming and nearly out of the limits of the tools which were provided for the build. It was decided that a forty-two inch octagon would be the final design of the diffuser sections exit.

The frame for the diffuser is very similar to the frame created for the contraction section. Though longer than the contraction section, four individual supports were created with the latter three, towards the exit side, having corner blocks installed to create and support the octagonal shape. Each of the supports were cut so that their internal angle would match the angle of expansion; providing ease of installation for the panels and higher rigidity, as proven during the construction of the contraction section. Also similar to the contraction section's frame, the supports were evenly spaced and connected together using horizontal bracing. The legs of the front two supports were affixed to one another through the use of horizontal braces, and the same was performed on the legs of the back two sections. These braces served the same function for the diffuser section as the horizontal braces for the contraction section, provide platforms on which the wheels, legs, and levelers were attached. Additional horizontal bracing was added between the second and third portions of the frame to increase rigidity during movement and assembly. Figure 3.18 below depicts the diffuser section's frame.

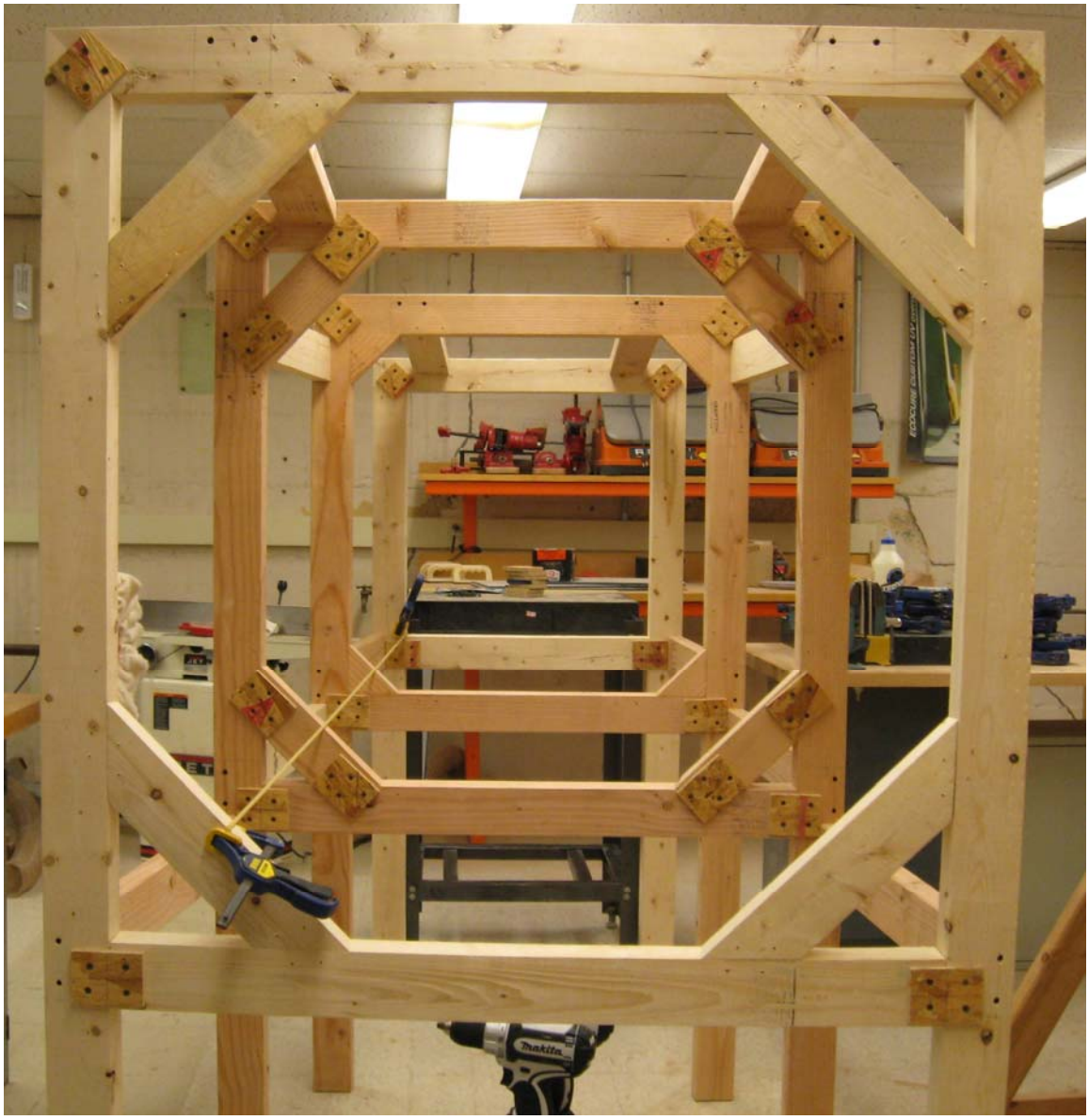

Figure 3.18 Diffuser section frame.

The octagonal design required the installation of four triangular panels, whose bases began at the exit end and terminate at the inlet side, and four trapezoidal panels, whose bases began at the inlet side and terminate at the exit end. All eight of these panels were constructed of the same ¼ inch thick plywood used to create the contraction section. The triangular panels were installed first and, similarly to the fitting method used in the contraction section, the trapezoidal

panels were cut to ensure a proper fit. Figure 3.19 below depicts the inside of the diffuser section once all of the panels were installed.

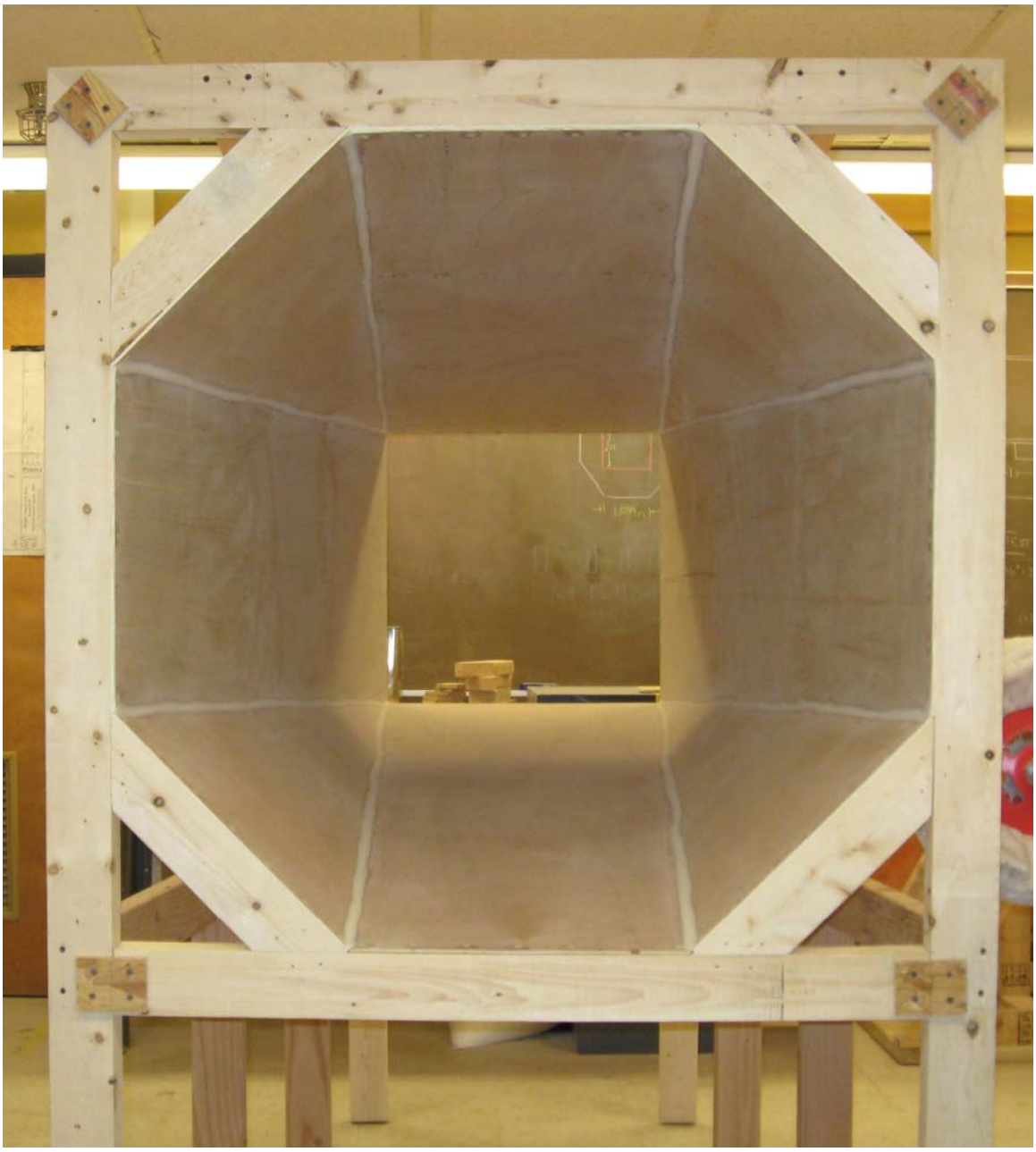

Figure 3.19 Inside of the diffuser section after panel installation.

Once all of the panels were attached to the frame, the same epoxy mixture as used in the contraction section was added. This mixture was able to reduce the amount of drag potential created by the holes for the fasteners and to provide a smooth transition between each individual piece comprising the body of the diffuser. A strip of the resin was added between each panel to prevent leakage. Finally, a coating of shellac infused with wax was placed inside of the section and hand sanded with steel wool to ensure laminar flow as the air exits the test section.

It was determined, after the fan and wheels were attached to the diffuser section, that the fan caused the center of gravity to become much higher and the wheels provided a fulcrum about which the diffuser could rotate. Therefore, a piece of 1018 cold drawn steel was affixed to the cross support placed between the legs of the entrance side of the diffuser frame. This piece of steel acted as a counter balance. A mild piece of steel was chosen as no loads or forces would be placed upon it. The dimensions for this ballast were 1.5 inches wide by 1.5 inches thick by twenty four inches long. With this volume, and the accepted density for steel taken from the 20th Edition of Machinery's Handbook, 0.284 pounds per cubic inch, approximately 15 pounds of force were added to the inlet side of the diffuser section (Schubert, Garratt, Semioli, & Moltrecht, 1979). Figure 3.20 below depicts this counter balance and its mounting.

Figure 3.20 Counterbalance affixed to the diffuser sections inlet support.

3.2.3. Fan

The fan used to power the tunnel is a simple and cost effective unit. In order in adhere to the budgetary restrictions of this thesis, while maintaining a feasible build time, a conventional forty-two inch shop fan was purchased. This fan, an Airmaster EMC42D, was chosen over the alternative of constructing a custom fan unit to power the tunnel. This unit was rated for a standard wall outlet of 120 volts alternating current, VAC, with an amperage draw of 4.5 amps. It is rated to move 14,000 cubic feet of air per minute, cfm, as listed by the manufacturer. The theoretical velocity calculations, based on the inlet dimensions of the test section, yield a velocity of 700 in/s. These calculations are shown below in Figure 3.21.

Fan Volumetric Ouput (cfm): $fo := 14000$

Test Section Area (ft^2): $tsa := 4$

Velocity (ft/min): $vf := \frac{fo}{tsa} = 3.5 \times 10^3$

Velocity (in/s): $vi := \frac{\left(\frac{fo}{tsa}\right)}{5} = 700$

Figure 3.21 Theoretical velocity calculations of flow within the test section based on the fan rating and test section inlet dimensions.

The fan unit was affixed to the exit side of the diffuser section. The fan is attached to the diffuser through means of carriage bolts and nuts, similar to the fashion in which the test section is attached to the contraction and diffuser sections. A support platform was added so that a single individual has the ability to assemble or disassemble the tunnel. Due to the large mass of the fan, the said individual would not have to support the full weight of the fan while loosening the fasteners. This support and fan are depicted below in Figure 3.22.

Figure 3.22 Fan and support platform as attached to the exit side of the diffuser section.

3.2.4. Screen

In order to ensure a laminar flow is present within the test section, a large polycarbonate screen was added to the front of the contraction section. This screen is able to straighten the air before it enters into the settling chamber. The dimensions of this screen were 66.5 inches wide by 66 inches tall with a thickness of 1.05 inches. The cell diameter was 0.270 inches with each cell having a wall thickness of 0.005 inches.

A two piece frame was constructed for the screen between which the screen was compressed. In order to reduce the chance of the screen becoming damaged, blocks having thicknesses of 0.090 inches were placed in the corners of the frame. Due to these blocks having been made slightly thinner than the screen, it allowed the screen to be secured, but not crushed.

The screen and frame were attached to the entrance of the contraction section through the means of four removable pin hinges, causing it to act as a door. Opposite the hinged side, two latches were placed so that the door would remain secure during disassembly, movement, and reassembly. This method of attaching the screen also allows the operator to easily access the internal portions of the contraction section when required. Due to the frame's large size and weight, it was found that it would sag when opened. To ensure proper placement when closed, a wedge was added to the bottom of the contraction section's first support. This wedged ensured that the screen would always return to a proper height after being closed and reduce the chance of turbulence being created by air flowing over the door's frame into the contraction section. Figure 3.23 below depicts the screen and its frame as attached to the entrance of the contraction section.

Figure 3.23 Screen and frame affixed to the front of the contraction section.

3.2.5. Computer and Data Acquisition System

Due to monetary restrictions placed on this thesis, a computer was not in the initial bill of materials and will not be included in the final cost analysis presented within this thesis. This section regarding the computer integration is merely to provide this researcher's insight and approach on the subject.

However, an integrated simple data acquisition unit was in the initial budget and will be included in the final cost analysis. Also covered in this section is the data acquisition systems integration into the overall design.

3.2.5.1. Computer

The computer integrated into this test apparatus was provided by Dr. Richard Mark French, associate professor in the department of Mechanical Engineering Technology at Purdue University in West Lafayette, Indiana. The monitor is a Dell 19 inch flat screen and the tower is a Dell Optiplex 755 with an Intel Core 2 Duo processor. In order to include them as part of the wind tunnel, the monitor was removed from its stand and a custom bracket was made. The tower was placed under the test section on the aforementioned platform in section 3.2.2 of this thesis. The tower was tightly secured to the test section stand's platform with nylon straps to prevent damage during movement.

Once the stand was removed from the monitor a custom plate and hangers were made so that the monitor would be able to be attached to the side of the contraction section closest to the researcher, yet remain removable. This bracket was comprised of three pieces. The first of which was a steel plate. The plate was made of 0.250 in thick steel and had overall dimensions of 4.75 inches by 4.75 inches. This plate was able to be attached to the monitor through the use of preexisting threaded holes in the back of the monitor. Affixed to this plate were two brackets of 0.125 inch thick steel which were bent so that they would allow the monitor to hang properly on the two by four frame. Figure 3.24 below is a depiction of the monitor as it would be in place during testing. The placement of the monitor allowed the individual using the tunnel to view real-time data provided by the program while being able to view the actual model as it was being tested. Figure 3.25 below depicts the plate and hangers which were made for the monitor. Since one of the requirements for this thesis is that the tunnel

remain modular and able to be transported, a cross brace was attached to the bottom of the test section's stand so that the monitor could be stored during transport without having to disassemble the computer system. Figure 3.26 below depicts the monitor in its secondary position which would be used during transport. This secondary position for the monitor is based upon the assumption that the test section would be moved while remaining up right only. If the test section must be placed on any of its sides, it is recommended that the entire computer system be removed.

Figure 3.24 Computer monitor attached to contraction section during tunnel operation.

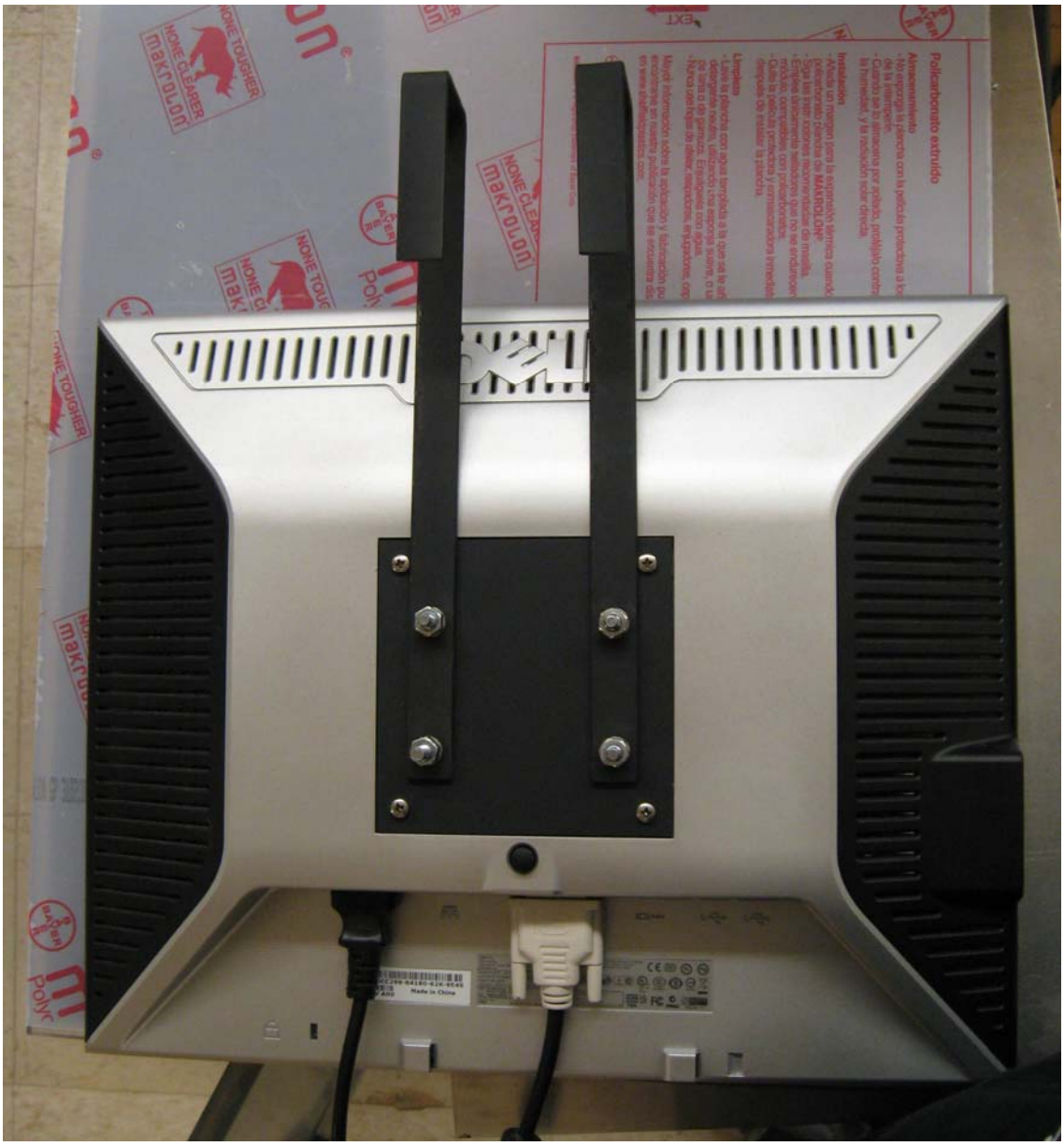

Figure 3.25 Custom bracket used in the integration of the computer monitor.

Figure 3.26 Monitor attached to the test section stand when the tunnel is not in operation.

3.2.5.2. Data Acquisition System

The purpose of including an integrated data acquisition system was so the individual using the apparatus would be able to connect their own laptop computer and collect data using a LabVIEW program. This LabVIEW program has been provided by the researcher so that accurate and automated measurements are made. Though the computer mentioned in the previous section has been included, the tunnel described in this thesis could be created so that only a computer must be added to record measurements.

The data acquisition unit and subsequent electronics, which will be covered in the next section of this thesis, were able to be mounted to the test section's stand along with the computer monitor. A separate panel was affixed to the stand which provided a mounting platform on which the DAQ and electronics package could be mounted.

3.3. Electronics

The instrumentation used to collect the empirical values was connected to a LabVIEW program. This program allowed the sample rates to be set equal and the accuracy of the values to be much greater than the accuracy of values as perceived by the researcher. The tunnel's pressure values were measured using a pitot tube connected to a Honeywell model DCXL01DS differential pressure sensor. The units for pressure measurements were initially recorded as inches of water (inH_2O) and converted by the researcher to pounds per square inch (psi). These values were converted to English units as the entire tunnel design and CFD analysis was carried out using English units. English units will be used for the entirety of the analysis.

In the original outline of this project, the flow temperature was to be measured using a flow meter equipped with a hotwire anemometer. However, due to the limitations of the CFD package, theoretical temperatures could not be calculated. Since the inclusion of an on-board electronics package, a simple thermocouple could be used to conduct these measurements. Also in the original outline, the same hotwire anemometer was to be used to measure the flow velocities. Due to the aforementioned monetary concerns, a hot-wire anemometer was not purchased and the flow velocities were derived with Bernoulli's equation using the pressure measurements obtained from the pitot tube and pressure sensor. These velocities were calculated in English units as inches per second (in/s).

3.3.1. Data Acquisition Unit

The initial DAQ which was to be integrated into the tunnel was a DATAQ 158-U. This unit was to be incorporated into a LabVIEW program with which the individual using the tunnel could make measurements. However, the inclusion of this device was abandoned due to severe complications and complexities involved in the integration with the National Instruments program. This device was initially chosen for its low price and ease of availability, but was later proven not to be as compatible or as robust as its more expensive replacement, National Instruments NI USB 6008. The incorporation of the DATAQ instrument within LabVIEW proved to be rather cumbersome and inefficient. Figure 3.27 below depicts the amount of programming required to perform a measurement using a strain gage adhered to an aluminum specimen and return the result to a waveform chart. It required the individual wishing to take measurements with the DATAQ device to know the virtual port location and the driver of the device; which could not be assigned a permanent port location due to its USB configuration.

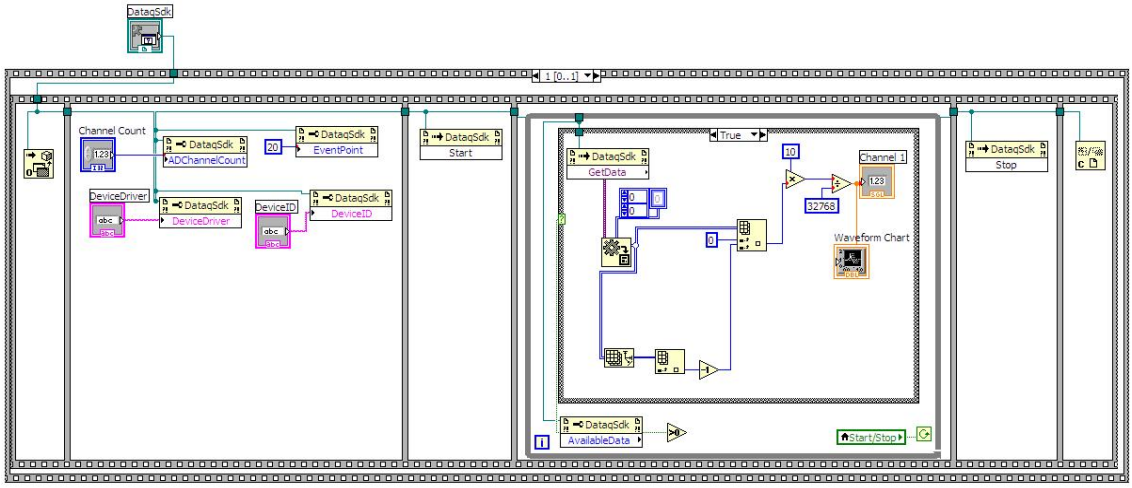

Figure 3.27 DATAQ 158-U data acquisition unit within National Instruments LabVIEW.

As mentioned the chosen replacement device for this thesis is the National Instruments NI USB 6008. This device is capable of allowing the user to perform plug-and-play measurements without having to know the devices communication port or driver; all of this is incorporated into the LabVIEW program. Therefore, the individual performing measurements is only required to install their measurement device and input its specifications. Figure 3.28 below depicts the amount of programming required to perform a measurement using a strain gage adhered to an aluminum specimen and return the result to a waveform chart. It is also noted that with the National Instruments device, the sample rate and amount of samples can be readily chosen and manipulated; two features which were unable to be controlled with the DATAQ device without driver modifications.

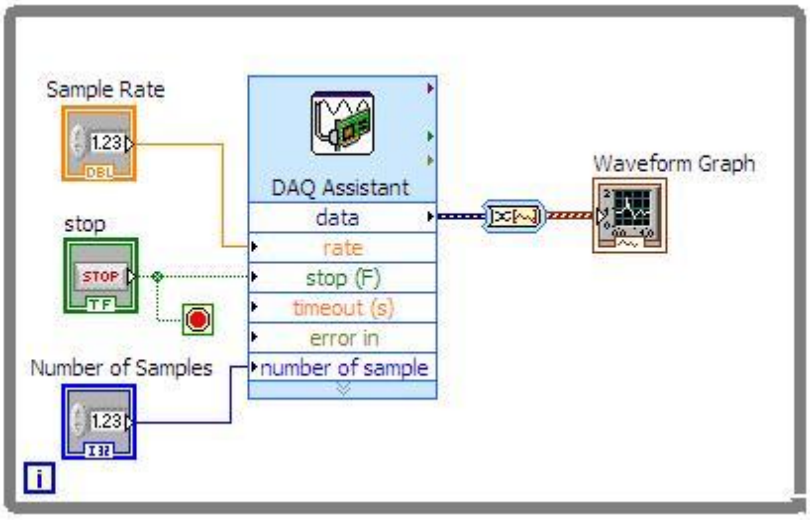

Figure 3.28 National Instruments USB 6008 data acquisition unit within LabVIEW.

Having chosen the National Instruments device as the better suited DAQ, this researcher was able to add further features to the controls of the wind tunnel. One such feature is the control of the fan through the use of a digital potentiometer. A DART, model 55AC01-21, rheostat was chosen to initially

control the fan unit, but was unable to provide precise control and velocities. Therefore, the potentiometer in the device from the manufacturer, DART, was removed and replaced with a potentiometer which could be digitally controlled through LabVIEW using the NI USB 6008. Since the testing of the tunnel was performed at full velocity, an overview of the programming required to control the fan via the digital potentiometer will not be given.

3.3.2. Sensors

As mentioned above, the sensor being used to collect differential pressure measurements was a Honeywell DCXL01DS. This sensor has an overall effective range of negative one inch of water to positive one inch of water and a linear error of ± 0.25% of the full scale span. The supply voltage for this sensor is 12VDC nominal with a low end limit of 3VDC and a maximum limit of 16VDC. Since this sensor is non-amplified, the output signal is proportional to the input voltage, leading to a full scale span of ten mill volts.

This researcher had first attempted to use a Honeywell ASDXRRX001PDAA5 differential pressure sensor which had a rating of negative one psi to positive one psi with an input requirement of 5VDC. This sensor was chosen first due to the much higher prices of sensors whose ranges were more sensitive to lower pressures. However, it was found that the ASDX model sensor was unable to detect and return the small pressure changes within the tunnel. It was found that the sensor’s amplification caused it to put out 2.5VDC nominally, thus leaving 2.5VDC for a positive one psi pressure and 2.5VDC for a negative one psi pressure. Due to this amplification, minute changes within the pressure of the tunnel did not have enough force to alter the output voltage enough for the researcher to determine if the values were signal noise or actual readings.

From hand calculations, it was found that the maximum overall pressure change within the tunnel during operation was 0.0275 psi. Figure 3.29 below contains this calculation. Using the specified transfer function provided by Honeywell for the ASDX model sensor, it was determined that the output voltage wall small enough that it could not be concluded that the values escaped the error and noise range of the sensor. At a maximum of 0.03 psi, the ASDX model sensor's change in voltage was 0.06VDC. Figure 3.30 below shows the transfer function for the ASDX model sensor and the subsequent output voltage obtained by incorporating the maximum theoretical pressure change within the tunnel.

Velocity (in/s): $v = 700$

Density of Air (lbm/in^3): $\rho := 0.0000433374$

Gravity (in/s^2): $g := 386.088$

Bernoullis Equation for Dynamic Pressure (psi): $q := \frac{1}{2} \cdot \frac{\rho}{g} \cdot v^2 = 0.028$

Figure 3.29 Maximum theoretical pressure changes within the test section based on fan specifications.

Bernoullis Equation for Dynamic Pressure (psi): $q := \frac{1}{2} \cdot \frac{\rho}{g} \cdot v^2 = 0.028$

ASDXRR001PDAA5 Transfer Function: $Vout := (2 \cdot q) + 2.5 = 2.555$

Ouput voltage minus nominal: $Vdiff := Vout - 2.5 = 0.055$

Figure 3.30 Output voltage of the ASDX sensor using the theoretical pressure values as shown in Figure 3.29 above.

Due to the unamplified output of the DCXL sensor, when zero pressure is applied, the output voltage is 0 VDC. This allowed for a full zero to ten mill volt output range for the pressure differential. The DCXL sensor also has a much higher resolution of one inch of water, 0.036psi. This value is much closer to the expected value changes and was able to provide results that were well out of the sensors noise range.

3.4. CFD Programming

Throughout this thesis, two forms of programming were used. The first type of programming performed utilized National Instruments LabVIEW which was briefly described in the section above. The second type of programming used was the CFD analysis which was performed to determine the theoretical flow values against which the tunnel would be tested. This CFD programming was performed using Algor provided by Autodesk. In order to obtain accurate results from the analysis, first an accurate model had to be created. This model, which is shown below in Figure 3.31, was created using Inventor by Autodesk. To ensure compatibility, the model was created and analyzed using programs from the same manufacturer. It is noted that only the inside portions of wind tunnel were precisely modeled. From these inner dimensions, an accurate fluid model was able to be created. Figure 3.32 below depicts the fluid modeling which was used to perform the CFD analysis.

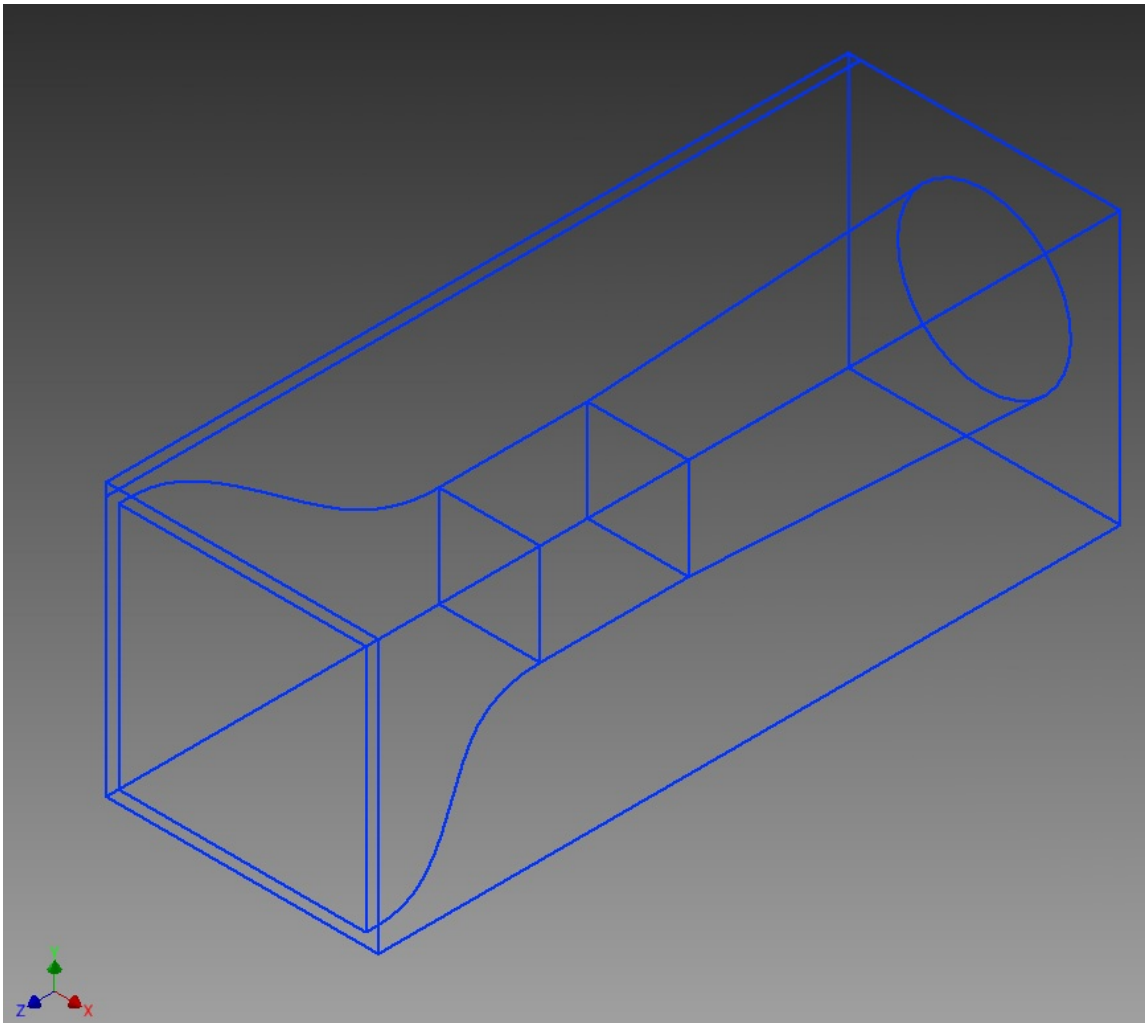

Figure 3.31 Model of the wind tunnel created using Inventor by Autodesk.

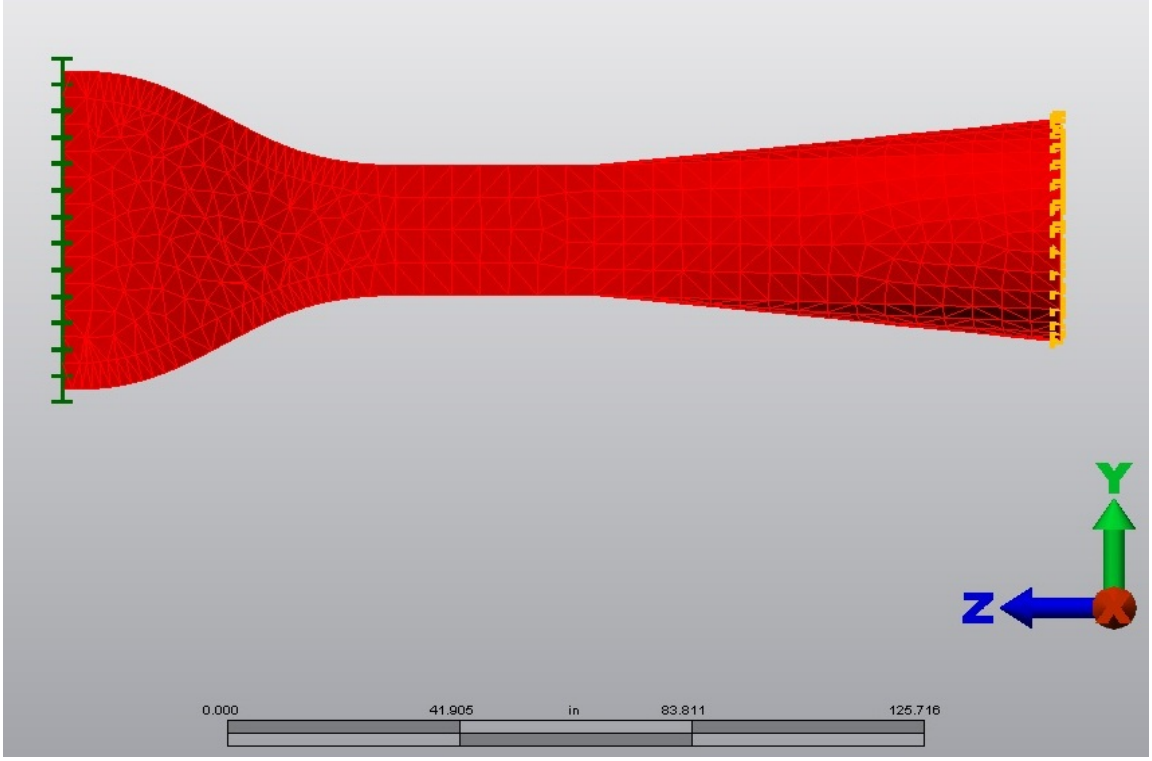

Figure 3.32 The fluid model used during the CFD analysis.

Once created, the fluid model was then meshed using a tetrahedral mesh to simulate fluid flow with boundary layer conditions. An inlet surface was specified so that the program would know where the fluid was allowed to enter and a fan surface was specified at the opposite end for fluid exit. Since the actual fan used in the construction of the tunnel has a rating of 14,000 cubic feet per minute, this value was converted into cubic inches per second and entered as 403,200. The direction of flow was indicated as being in the negative z direction. The initial wind tunnel model was created so that the x-axis ran through the center of the part. However, once imported into Algor, the program did not use the same origin orientation which had to be taken into account to ensure proper flow direction.

An initial loading profile was set and the simulation was to run as a steady state fluid analysis. However, after several failed attempts, the engineers at Autodesk suggested that the program be ran as an unsteady flow analysis. This unsteady analysis had to be performed due to fluctuations from the fan velocity as was simulated by the Algor software. It was stated by the engineers at Autodesk that since a fan face was specified, it would require much more time to compute a steady state flow and they were unsure if one could be reached within the program. Having made multiple attempts to create a load profile which would not ramp up to full speed too quickly, a successful unsteady flow analysis was achieved. Due to a steady state not being able to be reached, it was determined that once the unsteady state analysis was able to reach and maintain a common test section velocity, within a tolerance of plus or minus five inches per second, this data would be accepted as the true theoretical values.

3.5. Empirical Data Collection

Once having achieved a proper CFD program, a testing profile was set for the actual tunnel. During the collection period the tunnel was allowed to run and stabilize for a period of thirty seconds before the data collection process began. The allotted time of thirty seconds was determined by the CFD analysis as described in chapter 4 section 4.1. This waiting period was specified so that pressures and flow within the tunnel would be allowed to stabilize, reducing the possibility of collecting erroneous results. The LabVIEW program was set so that it would record fifty samples per second for a total of ten seconds, yielding five hundred data values per collection point. This sample rate was chosen because the flow patterns, theoretically, should not rapidly change. A higher sampling rate would not have yielded any finer results. These values were then written into a Microsoft Excel document so that they could be observed in their entirety. Each set of data collected from the individual points was averaged so that one value

would be yielded. This averaged value of each collection point was the value used in the analysis.

Points for measurement were chosen by taking the closest nodal points within the CFD program. Three planes were specified from which the data points would be taken. These planes are respectively listed as the test section and contraction section interface, the middle of the test section, and the test section and diffuser interface. The data was taken using a pitot tube connected to the aforementioned differential pressure sensor. The pitot tube was placed into the steam and held steady through the use of a small vise. If points were out of reach from the overall length of the pitot tube, as was the case for points near the top of the test section, a dowel rod was affixed to the pitot tube. Figure 3.33 below depicts the test set-up which was used to measure flow characteristics near the top of the tunnel.

Figure 3.33 Pitot tube used to take pressure measurements.

For the inlet and middle regions of the test section, the collection points were located by first setting the pitot tube's height, as measured from the top of test section. Secondly, the pitot tube was then positioned so that its dynamic pressure port would be flush with the desired plane, either the front or middle of the test section. In order to determine that the dynamic port was flush with each plane, a flat bar was placed across the plane's location and the pitot tube was moved to match. Finally, the distance from the back wall was measured and the placement of the pitot tube was set.

Due to the configuration of the diffuser section and the set up used to collect data the same procedure was not able to be used to collect the data for the exit portion of the test section. The same procedures were used to set the height of the tube and the distance from the back wall, however, instead of setting the dynamic pressure port to be flush with the exit plane, the static port was positioned so that it would become flush with the exit plane. This was done to ensure that the vise used to hold the pitot tube would remain level and so that the static pressure readings were obtained from the test section and not the diffuser section. Since pressures decrease within an object whose volumetric dimensions increase, as the case with the diffuser, it was determined by the researcher that no portion of the pitot tube should exit the test section.

Each point was tested twice at random and compared to the theoretical values gained from the CFD analysis. Chapter 4 below contains the individual data points, their locations, and their values. Also contained within Chapter 4 is an overall analysis of the conformity of the empirical results versus the theoretical values.

3.5.1. LabVIEW Programming

The LabVIEW program used for taking measurements during the empirical testing is very simple in concept. By utilizing the “DAQ Assistant” provided by National Instruments, the differential pressure sensor was assigned a channel and the maximum and minimum output values were set. Figure 3.34 contains a depiction of the ”DAQ Assistant” set-up page. Once the device was configured, its settings could be imported into LabVIEW. This feature allows the user to alter the sample rates, sample sizes, and output of the device.

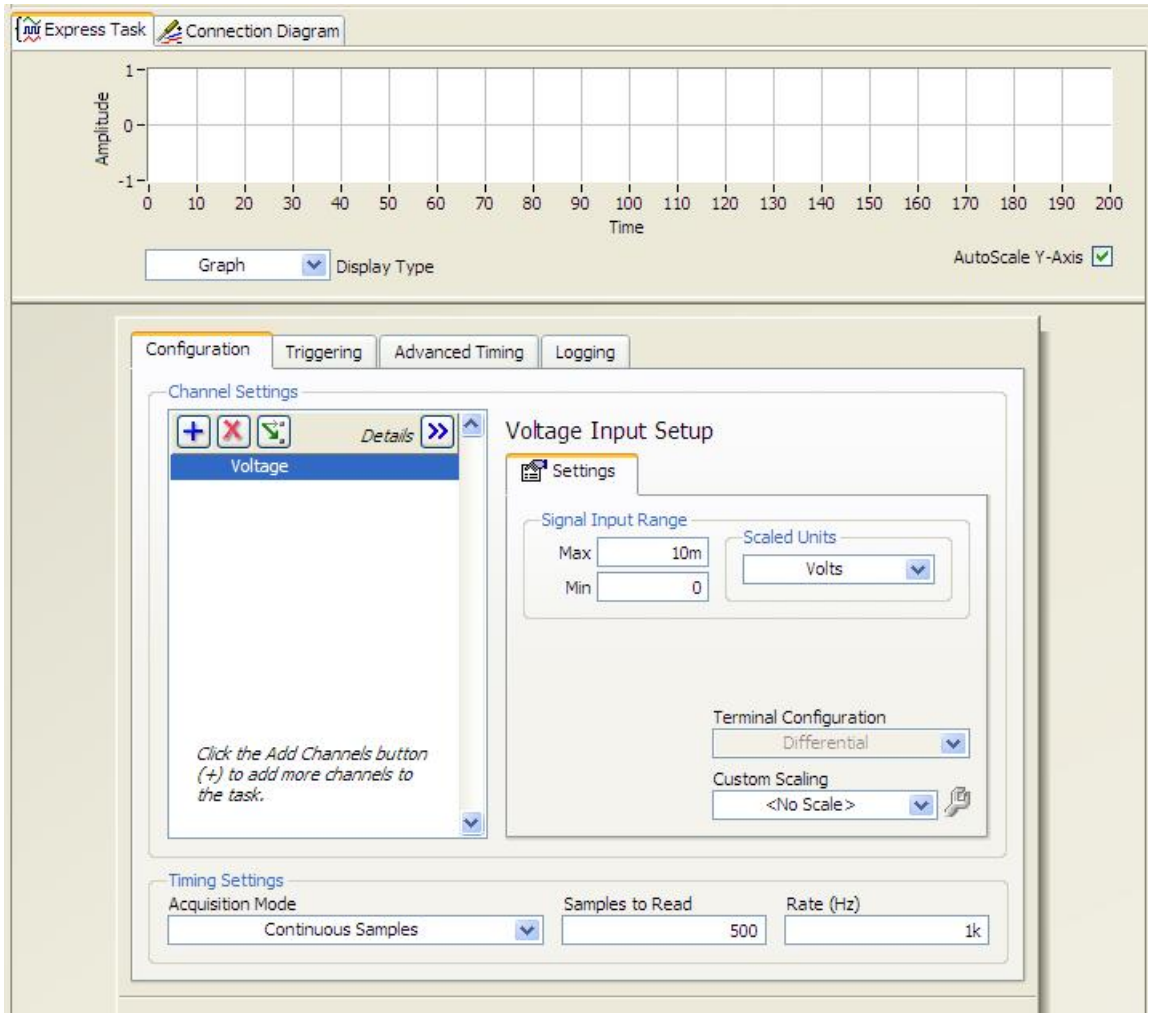

Figure 3.34 National Instruments DAQ Assistant set-up page.

The output of the device was split into three separate branches. Since the output was displayed as dynamic data, the first was converted into waveform data and used to produce a graph which the user could monitor. The second was converted into a double number and was written in its raw form to an excel spreadsheet. The third branch was altered using the conversion factors of the instrument and used to display the pressure and velocity readings for the user.

In order to write the second branch to a Microsoft Excel file, National Instrument's "write to spreadsheet" option was used. This option allows the user to specify the blank file, which must be created and saved ahead of time, and write their data to the file. The "write to spreadsheet" command allows for many options when programming. When creating the program, the researcher opted for the data to be written with as many decimal places as possible. It was also chosen that the data would erase the existing points within the spreadsheet and write the new values over them. This was done to ensure that continuous data streaming did not produce spreadsheets which were too large to be used. In order to ensure that relevant data was not lost, the user must save the file under a new name before performing the next set of tests. Figure 3.35 below contains a depiction of the block diagram of the programming performed for the empirical measurements. Figure 3.36 below contains a depiction of the front panel of the program used for the empirical measurements

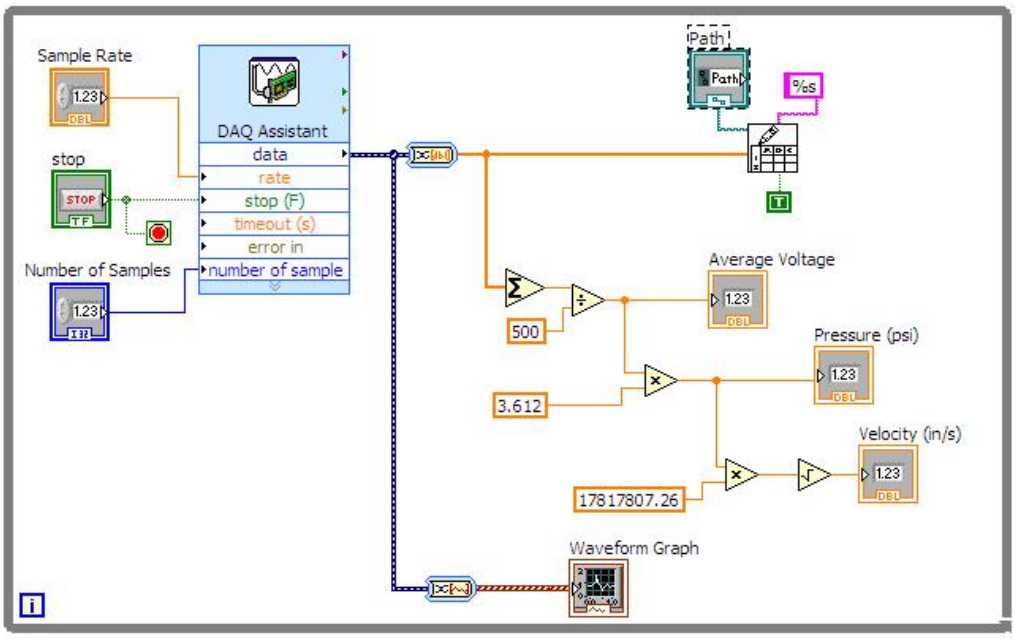

Figure 3.35 Block diagram programming used to take empirical measurements.

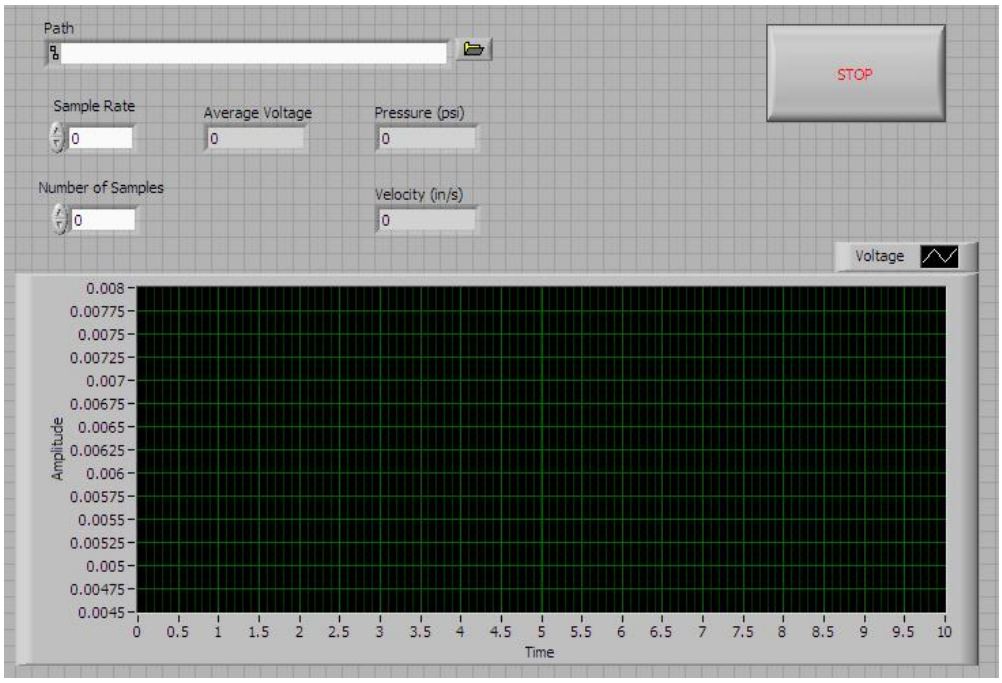

Figure 3.36 Front panel for the program used to take measurements. This front panel executes the programming displayed in Figure 3.35.

3.6. Statistical Method

For this thesis, the researcher has performed a quantitative statistical analysis. This analysis was based on a matched pairs t-test. A matched pairs design is able to compare the values assessed by one individual before a treatment to the values after a treatment. In the case of this analysis, the "individual" was each of the collection points taken from the CFD program. The velocities of these collection points, as given by the CFD program, were treated as the "before" values. The empirical values of the same collection points were then treated as the "after" values. The test determined the design's overall conformity between the two sets by taking the difference between the two values of each point, labeled V_{diff}, and performing a single sample t-test. The null hypothesis, H_o, was that $\mu_{diff} = 0$ and the alternative hypothesis, H_α, was that $\mu_{diff} \neq 0$. This comparison was performed using the Statistical Analysis Software (SAS) created by the SAS Institute Incorporated and provided by Purdue University. An alpha value of 0.05 was used in the determination of statistical significance.

Though three different regions of the tunnel were tested, an overall conformity of the tunnel to the theoretical results was desired. Thus, once all of the CFD and empirical results were collected, all of the data was lumped into one large analysis. At the onset of the analysis, it was unforeseen whether particular points within the computer model could be determined and whether replicating those points within the actual tunnel was possible. Once it was determined that a select amount of points were returned by the CFD program per chosen measurement plane, those points were matched as closely as possible by the researcher and a matched pairs test was performed.

The results of this matched pairs test can be found in chapter 5 section 5.2 below. The individual points and their associated velocities, as give by the CFD program, can be found in chapter 4 section 4.2 below. The corresponding points measured from the tunnel can be found in chapter 4 section 4.3 below.

3.7. Summary

This section of the thesis has contained the construction of the wind tunnel, a description of the data acquisition hardware and sensors used to take empirical data, a description of the CFD programming used to determine theoretical data, and the statistical methodology which was used to compare the theoretical results to the empirical results.

CHAPTER 4. PRESENTATION OF DATA

4.1. Introduction

This section of the thesis will present the data collected during the computational fluid dynamic analysis and the data collected from the empirical testing. The statistical comparison of the data points as well is a brief budgetary analysis can be found in chapter 5 below.

4.2. Computational Fluid Dynamics Data

As described in the previous chapter a steady state computational fluid dynamics, CFD, analysis was unable to be performed due to the large amount of time which would have been required. Therefore, an unsteady state CFD analysis was performed. This analysis was programmed so that it would run for enough time to allow the reactions within the tunnel to stabilize within a tolerance of plus or minus five inches per second within the test section. This tolerance was set by the researcher as an acceptable amount of variation based upon the theoretical maximum velocity within the test section calculated from the dimensions of the test section and the fan's maximum rated volumetric flow rate, 14,000 cfm. This value was obtained from the data sheets provided by the manufacturer, Airmaster. Since the maximum theoretical flow, calculated from the fan's specifications was 700 inches per second, a total tolerance of ten inches per second yielded an approximate 1.4 percent difference.

From the CFD analysis, it was determined that the tunnel would reach a point of semi-steady flow, which adhered to the set tolerance, after approximately thirty seconds of operation. After such time, the flow within the test section varied by one to two inches per second, which is lower than the overall set tolerance. The maximum theoretical flow within the test section, as found by the CFD analysis was 720 inches per second. This maximum value was found at the front of the test section 0.50 inches away from the top wall and 11.75 inches away from the back wall. This maximum velocity is approximately 2.86 percent higher than the theoretical maximum flow found from the fan's specifications. This flow is likely higher due to an under-rating of the fan's capabilities by the manufacturer. Figures 4.1 and 4.2 below depict the velocity and pressure profiles respectively, captured from the CFD analysis. Figure 4.3 depicts a particle stream placed within the flow using the CFD results. This particle stream does not present any evidence of turbulent flow within the test section. Figure 4.4 below depicts a view of the theoretical boundary layer as found within the corners of the test section.

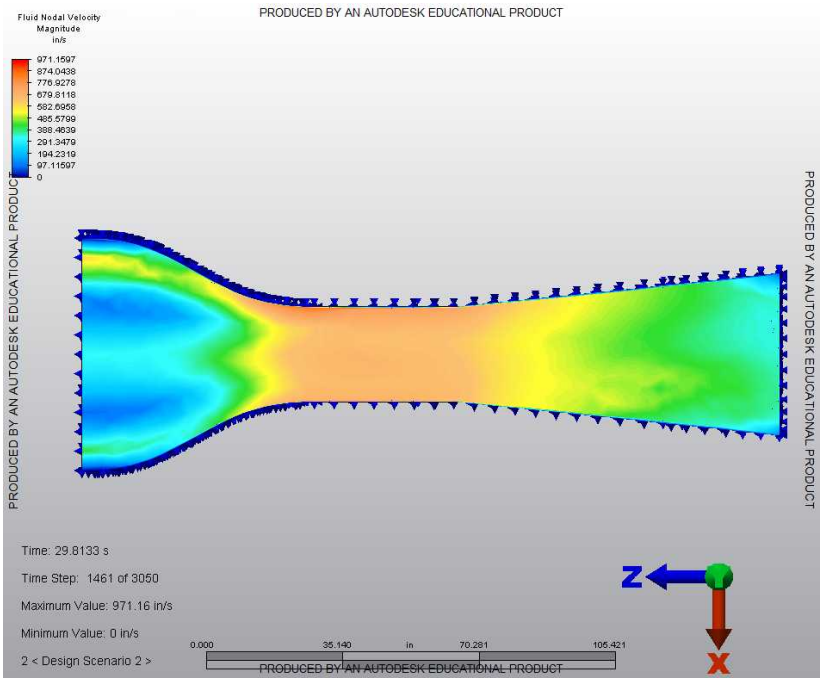

Figure 4.1 Screenshot of the velocity profile taken from the CFD program.

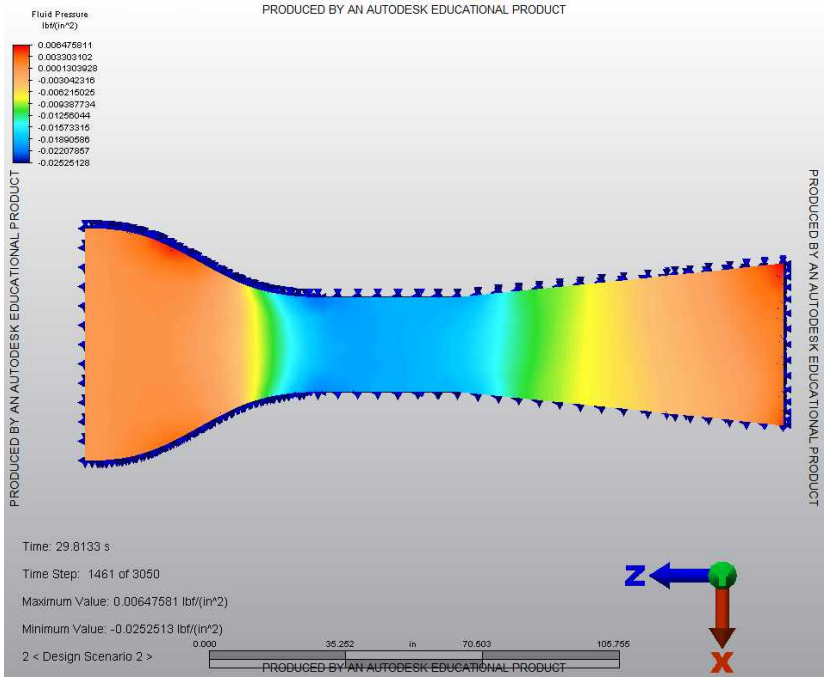

Figure 4.2 Screenshot of the pressure profile taken from the CFD program.

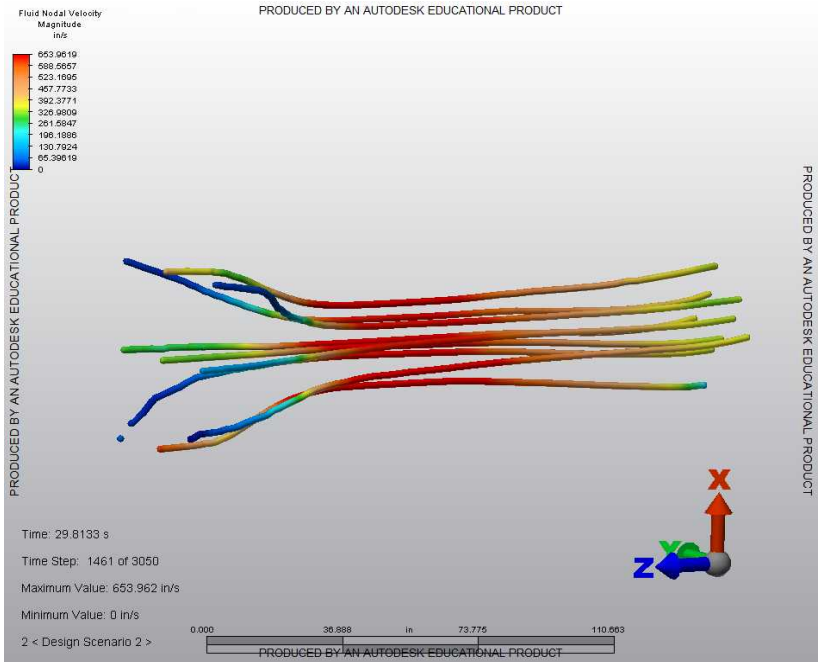

Figure 4.3 Screenshot of a particle flow within the tunnel.

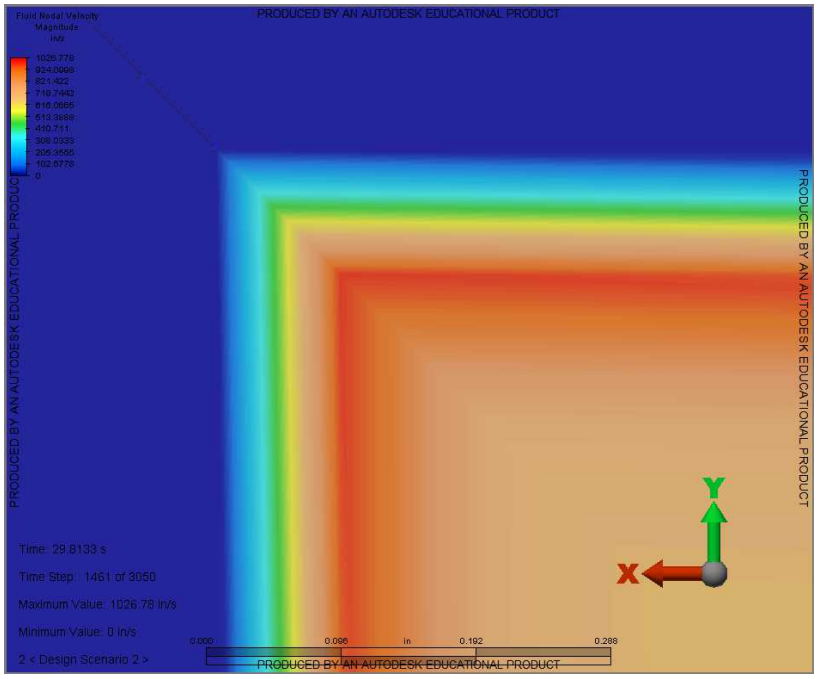

Figure 4.4 Screenshot of the boundary layer build-up within the middle of the test section.

The CFD theoretical flow through the center point of the front of the test section was found to be approximately 595 inches per second. The CFD center point flow within the middle, 1.5 feet away from the inlet, of the test section was found to be approximately 654 inches per second. At the exit of the test section, the CFD center point flow was found to be approximately 643 inches per second.

Individual collection points within the flow for each of the three regions used for analysis were difficult to place. While the Algor program has the ability to determine the velocity at any point within the flow, it does not give the user the coordinates which correspond to the velocities. Therefore, the researcher was limited to using the nodal points which were set by the program during the analysis. These nodal points were able to provide the velocity, as well as the x and y coordinates of the points. Since the tunnel is axisymmetric about the x and y axes, the researcher chose to divide the tunnel into four sections and obtain values for one of the quadrants. Tables 4.1, 4.2, and 4.3 below depict the nodal

points chosen for each region of testing. Given within these tables are the point numbers, the velocities at those points, and the location of the points as measured in inches from the top and back walls. The researcher chose to measure the distance from the walls rather than the origin since no actual reference origin exists within the tunnel. Measuring the distances from the walls provided an actual surface which could be referenced. Also shown below in Figures 4.5, 4.6 and 4.7 are screenshots of the respective regions of data collection taken from the CFD analysis results.

Table 4.1 *Front of test section CFD data*

Point	Distance from back wall (in)	Distance from top wall (in)	Velocity (in/s)
1	0.0885	0.0885	338.27
2	0.1948	0.1948	578.228
3	0.3233	0.3233	696.20
4	3.139	3.021	672.561
5	6.125	0.125	641.958
6	6.125	0.4558	700.25
7	7.026	3.805	647.044
8	6.087	7.634	607.669
9	11.75	0.4558	720.717
10	11.375	3.971	632.971
11	11.75	11.75	594.608

Table 4.2 *Middle of test section CFD data*

Point	Distance from back wall (in)	Distance from top wall (in)	Velocity (in/s)
1	11.75	11.75	654.239
2	5.882	5.540	647.100
3	8.430	10.386	637.636
4	10.976	4.994	647.349
5	8.893	6.704	645.003
6	4.306	8.398	639.366
7	8.544	11.189	674.562

Table 4.3 *Exit of the test section CFD data*

Point	Distance from back wall (in)	Distance from top wall (in)	Velocity (in/s)
1	4.901	0.4554	678.012
2	6.877	3.544	658.866
3	9.927	6.199	634.914
4	3.730	6.610	674.872
5	11.023	10.218	631.316
6	5.960	10.075	650.034
7	0.4552	9.8	715.181
8	11.75	11.75	642.505

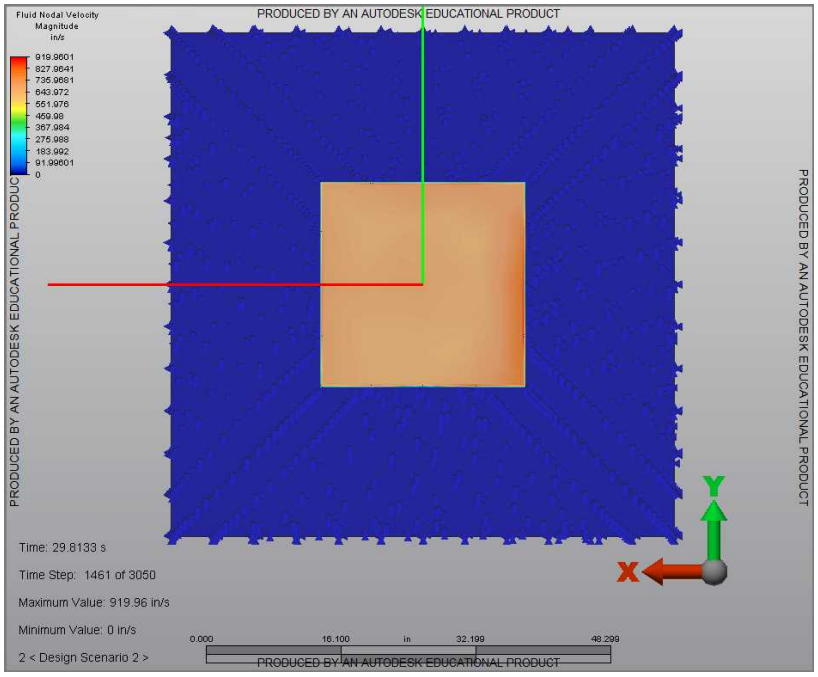

Figure 4.5 Screenshot of the test section inlet velocities.

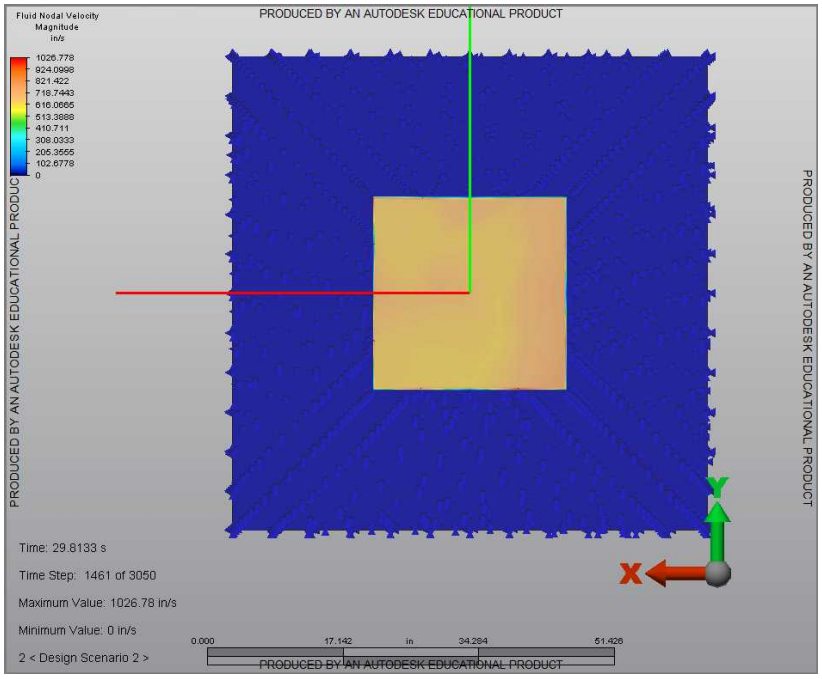

Figure 4.6 Screenshot of the test section middle velocities.

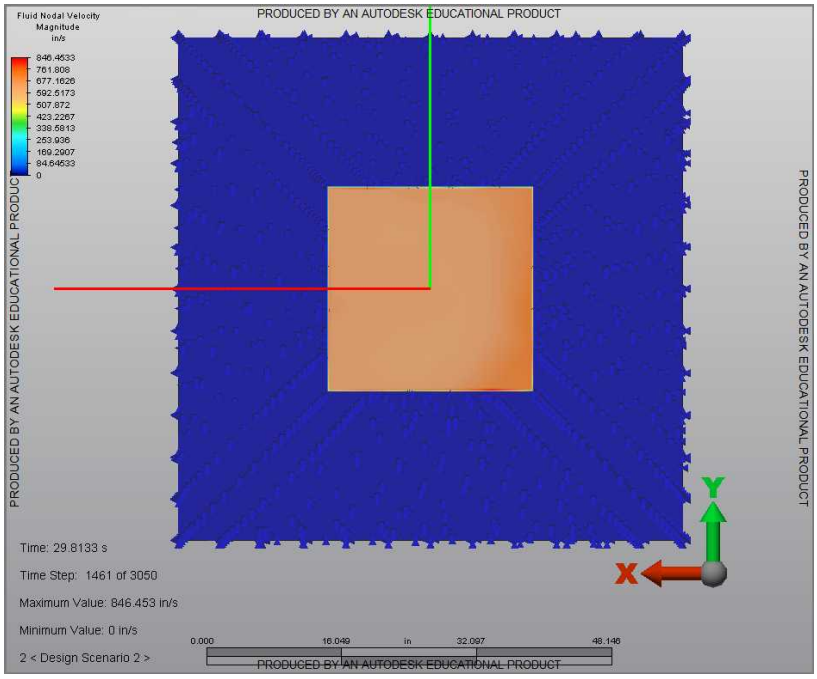

Figure 4.7 Screenshot of the test section exit velocities.

Once all of these points were collected and cataloged, they were approximately matched within the tunnel and measured by empirical means. This matching and the subsequent data are found in the section below.

4.3. Empirical Testing Data

Once the points for measurement were found from the CFD programming, the researcher attempted to locate the points within the actual tunnel. Determining each location was performed using conventional shop tools, as large precision devices were not available to the researcher. The determination of the location of these points was described in section 3.5 above. Due to the equipment which was used to locate the points within the actual flow were not precisely accurate, the locations were rounded to the nearest 1/16th of an inch.

The maximum actual velocity measured within the tunnel was measured at the inlet of the test section. This point was located 0.50 inches from the top plate and 6.125 inches from the back wall and had a velocity of approximately 701 inches per second. Using 741 miles per hour as the accepted speed of sound at sea level, as provided by Wong (1986), this leads to a Mach number of approximately 0.054 for the tunnel. This maximum velocity is approximately 0.14 percent higher than the theoretical maximum velocity calculated using the fan's specifications, 700 inches per second, and approximately 0.14 percent higher than that point's corresponding CFD theoretical value, 700.25 inches per second. Tables 4.4, 4.5, and 4.6 below give the points measured within the actual tunnel flow. The velocities and distances from the top and back walls are listed as well.

Table 4.4 *Empirical data from test section inlet*

Point	**Distance from back wall (in)**	**Distance from top wall (in)**	**Velocity (in/s)**
1	0.0625	0.0625	401.901
2	0.1875	0.1875	599.087
3	0.3125	0.3125	666.117
4	3.125	3	628.482
5	6.125	0.125	649.542
6	6.125	0.50	701.13
7	7.0	3.8125	632.1
8	6.0625	7.625	631.393
9	11.75	0.50	699.119
10	11.375	4.0	626.812
11	11.75	11.75	625.662

Table 4.5 *Empirical data from test section middle*

Point	Distance from back wall (in)	Distance from top wall (in)	Velocity (in/s)
1	11.75	11.75	642.65
2	5.8125	5.5625	623.46
3	8.4375	10.375	643.922
4	11.0	5.0	625.191
5	8.875	6.6875	636.557
6	4.3125	8.375	624.876
7	8.5625	11.1875	653.312

Table 4.6 *Empirical data from test section exit*

Point	Distance from back wall (in)	Distance from top wall (in)	Velocity (in/s)
1	4.875	0.50	627.439
2	6.875	3.5625	639.329
3	9.9375	6.1875	631.859
4	3.375	6.625	607.554
5	11.0	10.25	631.185
6	6.0	10.0625	634.651
7	0.50	9.8125	550.673
8	11.75	11.75	622.146

Using the equation depicted below in Figure 4.8, a Reynolds number of approximately 737200 was calculated for the tunnel. This value was calculated using the maximum actual flow velocity within the test section, 701.13 inches per second (58.428 ft/s), the width of the test section, 2 feet, and 0.0001585 feet squared per second as the kinematic viscosity of air. This kinematic viscosity

value was obtained from Turns and Kraige (2007), assuming a temperature of 520 degrees Rankine, 60 degrees Fahrenheit.

Maximum Actual Velocity (ft/s): $Vmax := 58.428$

Test section width (ft): $Tw := 2$

Kinematic Viscosity (ft^2/s): $v := 0.0001585$

Reynolds Number Calculation: $R := \frac{(Vmax \cdot Tw)}{v} = 7.373 \times 10^5$

Figure 4.8 Reynolds number calculations.

CHAPTER 5. RESULTS, CONCLUSION, AND DISCUSSION

5.1. Introduction

This chapter contains the statistical comparison of the data points listed in chapter 4 sections 4.2 and 4.3. This comparison uses a matched pairs t-test with an alpha value of 0.05. A brief budgetary analysis of the tunnel, conclusion, and discussion of future research is listed as well.

5.2. Statistical Analysis of Data

The analysis below was performed using Statistical Analysis Software, SAS, from SAS Institute Incorporate provided to the researcher by Purdue University. The data obtained from the computational fluid dynamics, CFD, programming was statistically compared to the actual values obtained from the tunnel through the use of a pitot tube and a differential pressure sensor. These values were compared using a matched pairs t-test with an alpha value of 0.05. The CFD results were treated as the “before” values and the empirical results were treated as the “after” values. Therefore, the empirical values were subtracted from the CFD values to obtain the value V_{diff}, which was used to perform a one sample t-test.

In order to determine if the data would be able to be used in the analysis, two quantile plots were created to determine the linearity of the data of the first and second rounds of empirical testing. The first quantile plot contains the data collected during the first empirical tunnel analysis. This plot, shown below in Figure 5.1, shows evidence of a semi linear fit. However, two different items were

of concern. The first of which is a slight curvature of the points present near the end of the line. The second item of concern is a drastic outlier, located on the far right end of the plot. This outlier was found within the data sets as the point specified as having a theoretical velocity of approximately 715 inches per second, yet having a measured velocity of approximately 551 inches per second. This point was measured at the interface between the outlet of the test section and the inlet of the diffuser section. This point, as specified by the CFD program, is a clear anomaly as it presents a very high velocity within the boundary layer of the test section. Though it may be an anomaly within the CFD analysis, this is not grounds on which the point may be thrown out statistically. In order to determine if this point was a true influential value, a secondary quantile plot was created without the suspect value. This second plot is much more linear and contains nearly the correct forty five degree angle required for the data to be considered normally distributed. This second quantile plot can be found in Figure 5.2 below.

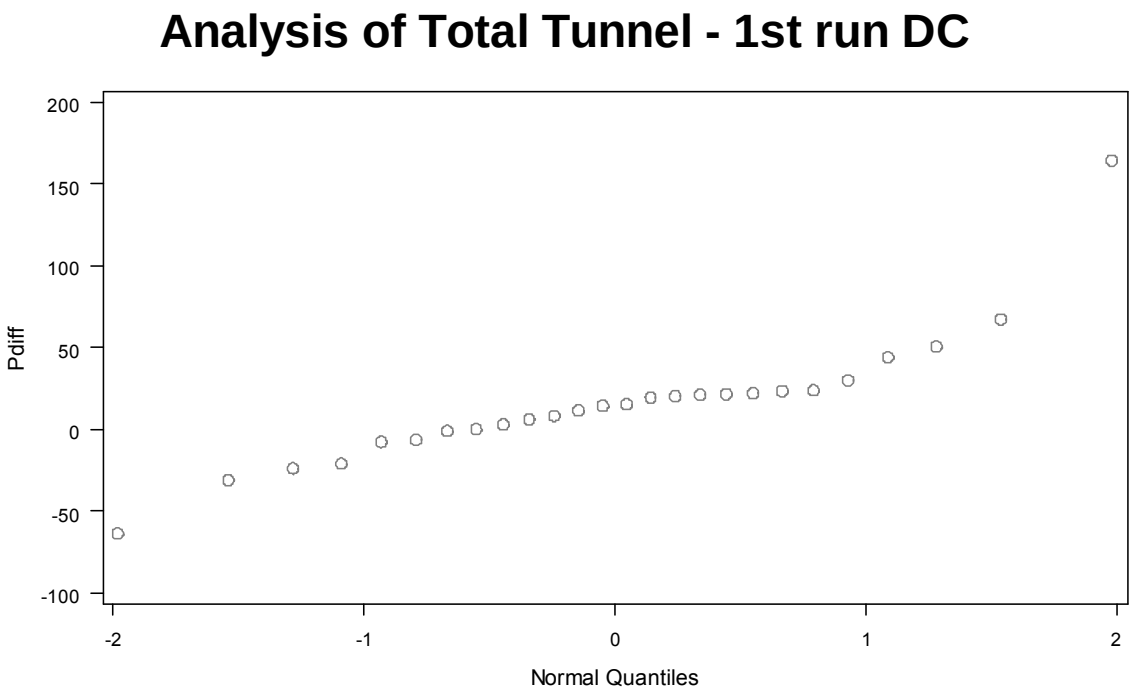

Figure 5.1 Quantile plot created from the first run of empirical testing.

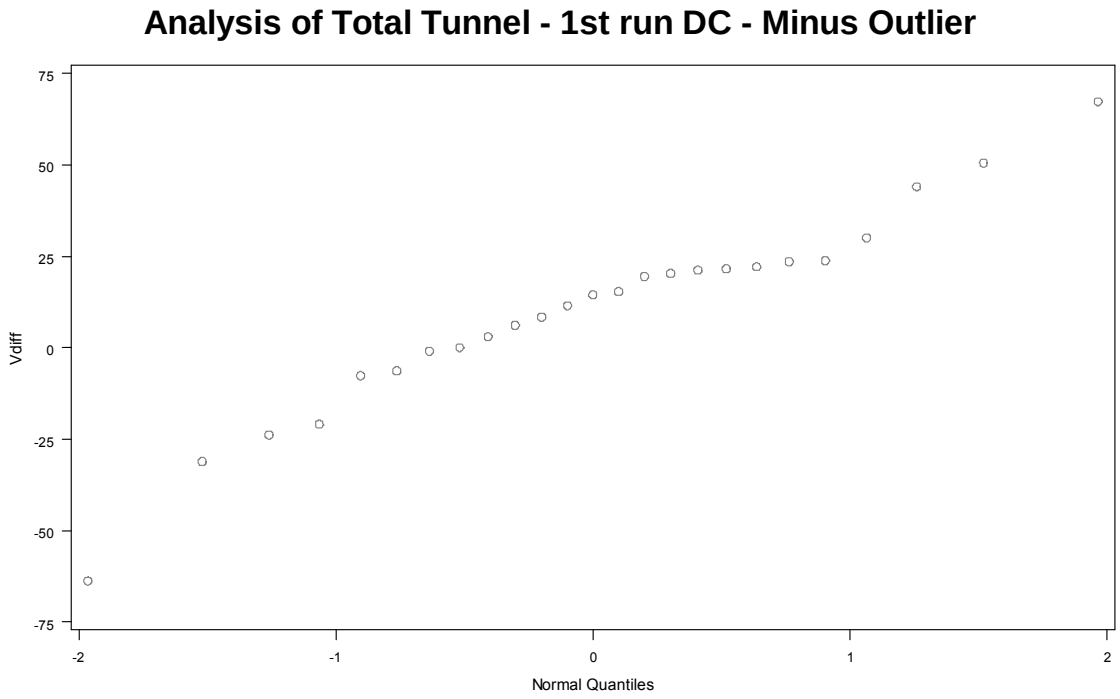

Figure 5.2 Quantile plot created from the first run of empirical testing, excluding the suspect point.

Once the quantile plots for the first run were examined, the matched pairs t-tests were carried out using the two data sets; the first containing the outlier and the second without. Figure 5.3 below contains the SAS output from the first test containing the suspect point. From this test, it was found that a probability value of 0.0545. This probability allows the researcher to accept the null hypothesis and conclude that the actual values obtained from the tunnel are not significantly statistically different. Therefore, it can be said that the tunnel adheres to the CFD model. The second analysis was performed on the set of data obtained during the first empirical run, excluding the suspect data point. This statistical analysis provided a probability of 0.0774. This probability also allows the null hypothesis to be accepted. Figure 5.4 below contains the SAS output from the second test without the outlier.

Analysis of Total Tunnel - 1st run DC

The UNIVARIATE Procedure

Variable: Pdiff

Basic Statistical Measures

Location		Variability	
Mean	15.92892	Std Deviation	40.26248
Median	14.93620	Variance	1621
Mode	.	Range	228.08103
		Interquartile Range	24.52023

The TTEST Procedure

Difference: CFD - empirical

N	Mean	Std Dev	Std Err	Minimum	Maximum
26	15.9289	40.2625	7.8961	-63.6310	164.5

Mean	95% CL Mean		Std Dev	95% CL Std Dev	
15.9289	-0.3334	32.1913	40.2625	31.5761	55.5787

DF	t Value	Pr > |t|
25	2.02	0.0545

Figure 5.3 SAS output for the set first empirical data collection.

Analysis of Total Tunnel - 1st run DC - Minus Outlier

The UNIVARIATE Procedure

Variable: Vdiff

Basic Statistical Measures

Location		Variability	
Mean	9.98807	Std Deviation	27.06922
Median	14.48983	Variance	732.74254
Mode	.	Range	130.94902
		Interquartile Range	23.03796

The TTEST Procedure

Difference: CFD - empirical

N	Mean	Std Dev	Std Err	Minimum	Maximum
25	9.9881	27.0692	5.4138	-63.6310	67.3180

Mean	95% CL Mean		Std Dev	95% CL Std Dev	
9.9881	-1.1856	21.1617	27.0692	21.1364	37.6574

DF	t Value	Pr > |t|
24	1.84	0.0774

Figure 5.4 SAS output for the set of data obtained during the first empirical data collection, excluding the suspect point.

The second set of empirical testing data was examined as well using the same procedures for the first set. Since the same CFD values were used, the same suspect point presents itself. Therefore, as was performed with the first set of empirical data, quantile plots and analyses were performed with and without the suspect CFD value. Figures 5.5 and 5.6 below contain the quantile plots and their associated SAS outputs. The analysis which included the suspect point yielded a probability of 0.0595. The analysis which excluded the suspect point yielded a probability of 0.0832. Both of these sets also allow for the null hypothesis to be accepted.

Analysis of Total Tunnel - 2nd run DC

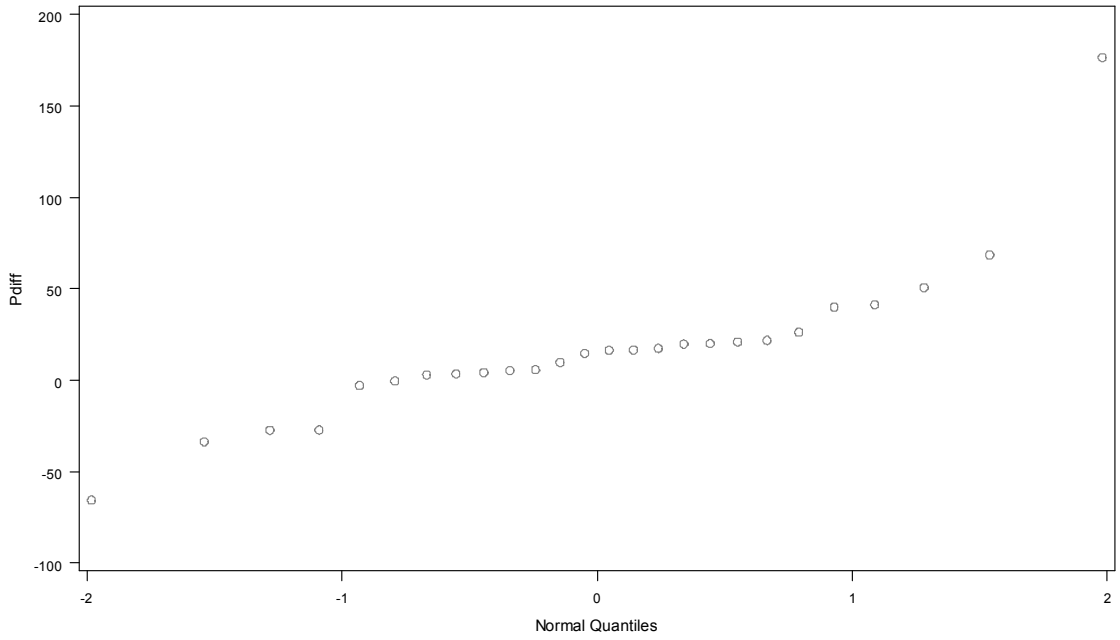

Analysis of Total Tunnel - 2nd run DC

The UNIVARIATE Procedure

Variable: Pdiff

Basic Statistical Measures

Location		Variability	
Mean	16.48023	Std Deviation	42.56201
Median	15.63728	Variance	1812
Mode	.	Range	241.95203
		Interquartile Range	18.69844

The TTEST Procedure

Difference: CFD - empirical

N	Mean	Std Dev	Std Err	Minimum	Maximum
26	16.4802	42.5620	8.3471	-65.4200	176.5

Mean	95% CL Mean		Std Dev	95% CL Std Dev	
16.4802	-0.7109	33.6714	42.5620	33.3796	58.7530

DF	t Value	Pr > |t|
25	1.97	0.0595

Figure 5.5 Quantile plot and SAS output for the second run of empirical data collection.

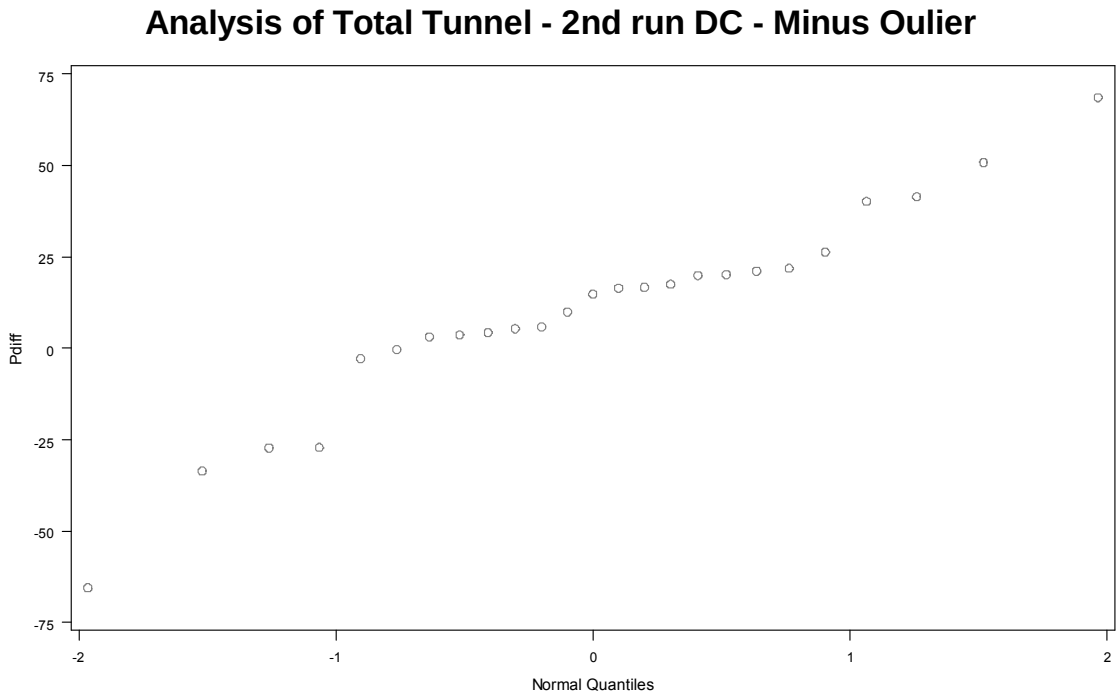

Analysis of Total Tunnel - 2nd run DC - Minus Oulier

The UNIVARIATE Procedure

Variable: Pdiff

Basic Statistical Measures

Location		Variability	
Mean	10.07815	Std Deviation	27.87388

Median	14.80383	Variance	776.95343
Mode	.	Range	133.97902
		Interquartile Range	17.97021

The TTEST Procedure

Difference: CFD - empirical

N	Mean	Std Dev	Std Err	Minimum	Maximum
25	10.0782	27.8739	5.5748	-65.4200	68.5590

Mean	95% CL Mean		Std Dev	95% CL Std Dev	
10.0782	-1.4276	21.5839	27.8739	21.7647	38.7768

DF	t Value	Pr > |t|
24	1.81	0.0832

Figure 5.6 Quantile plot and SAS output for the second run of empirical data collection, excluding the suspect point.

5.3. Budgetary Analysis

The budgetary analysis performed on this project is given below. A total sum of less than 6000 dollars was allotted for the build and testing. The computer, which was donated to the project, has not been included. Also, the computer and software which were used to perform the CFD analysis have not been included, as those were used to validate the design and are not part of the apparatus. Table 5.1 below gives a breakdown of the funds used.

When viewing the results of the budgetary analysis, it can be seen that the total material costs were under half of the total allotted budget. It is noted that the final value listed in the table below only contains the monetary expenditures for building and testing supplies; no labor costs have been recorded.

Table 5.1 *Budgetary analysis of the tunnel*

Vendor	**Amount (dollars)**
Amazon	122.49
National Instruments	167.43
MSC	1,276.97
Grainger	128.88
Aircraft Spruce & Specialty	153.71
McMaster-Carr	323.63
Menards	66.30
Von Tobel	76.50
Ace Hardware	193.22
Allied Electronics	101.47
Central Machine Shop	150.00
Fastenal	29.55
Total	**2790.15**

5.4. Conclusion

Given the data and the statistical analysis of the tunnel, it can be concluded that the overall design does adhere to the theoretical values. Therefore, it can be said that this type of design is successful in producing adequate laminar flows within the test section. When examining the allotted budget, it can also be concluded that the tunnel was able to be built well within the means of a university laboratory budget.

Finally, it is also recommended by the researcher that the blades within the fan unit of the tunnel be refined. Since this fan is designed for moving air through shops and garages, the blade angles and chord lengths do not match the optimum values required for steady wind tunnel operation.

5.5. Discussion

In regards to further analysis and research to be performed on the tunnel, it would be wise for a full boundary layer mapping to be performed. Though it is understood and accepted that the tunnel was able to match theoretical values, the boundary layer conditions within the test section should be examined to ensure that a large build-up is not occurring. Such a build-up could cause pressures within the test section to increase, allowing for artificial lift conditions to be presented. While it is not believed that the boundary layer is becoming large enough to separate within the test section, a proper assurance would allow for increased certainty within the values collected from the tunnel during testing.

LIST OF REFERENCES

LIST OF REFERENCES

Blazewicz, M., Kurowski, K., Ludwiczak, B., Napierala, K. (2010). Problems related to parallelization of CFD alorithms on GPU, multi-GPU and hybrid architectures. *AIP Conference Proceedings, 1281*(1), 1301-1304.

Chamorrow, L. P., & Porte-Agel, F. (2010). Effects of thermal stability and incoming boundary-layer flow characteristics on wind-turbine wakes: a wind-tunnel study. *Boundary-Layer Meteorology, 136*, 515-533. doi: 10. 1007/s10546-010-9512-1

Curle, N. (1962). The laminar boundary layer equations. London: Oxford University Press.

Hoske, M. T. (2009). Benchtop windtunnels: Calibration, thermal analysis. *Controls Engineering,* (7), 56.

Howell, R., Qin, N., Edwards, J., Durrani, N. (2010). Wind tunnel and numerical study of a small vertical axis wind turbine. *Renewable Energy, 35*, 412 – 422.

Kubesh, R. J., & Allie, B. W. (2009). A wind tunnel for an undergraduate laboratory. *International Journal of Mechanical Engineering Education, 37*(1), 21-26.

Lan, C. E.,& Roskam, J. (1981). Airplane aerodynamics and performance. Ottawa, Kansas: Roskam Aviation and Engineering Corporation.

Laurentiu, N. (2004). Modeling and simulating engineering processes with computational fluid dynamics. *JOM, 53*(3), 43.

Mecham, M. (2003). Big wind no more. *Aviation Week & Space Technology, 158*(21), 40.

NASA Investigating Tunnel Safety. (2001). *Aviation Week & Space Technology,154*(19), 65.

Pankhurst, R. C., & Holder, D. W. (1952). Wind-tunnel technique. New York, New York: Pitman Publishing Corporation.

Pope, A. (1954). Wind-tunnel testing. New York, New York: John Wiley & Sons, Incorporated.

Rae, W. H., & Pope, A. (1984). Low-Speed Wind Tunnel Testing. New York, New York: John Wiley & Sons, Incorporated.

Schlichting, H. (1960). Boundary Layer Theory. New York, New York: McGraw Hill Book Company, Incorporated.

Schubert, P. B., Garratt, G., Semioli W. J., Moltrecht, K. H. (20th Ed.). (1979). *Machinery handbook: a reference book for the mechanical engineer, draftsman, tool maker, and machinist.* New York, New York: Industrial Press Incorporated.

Smith, S. (2002). Recent advances in digital data acquisition technology. *Sound and Vibration, 36*(3), 18-21.

Studt, T. (2004, March). CFD & wind tunnels reverse roles. *R&D Magazine, 46*(3), 19-21.

Turns, S. R., Kraige, D. R. (2007). *Property tables for thermal fluids engineering*. New York, New York: Cambridge University Press.

Wong, G. S. K. (1986). Speed of sound in standard air. *Journal of the Acoustical Society of America, 79*(5), 1359-1366.